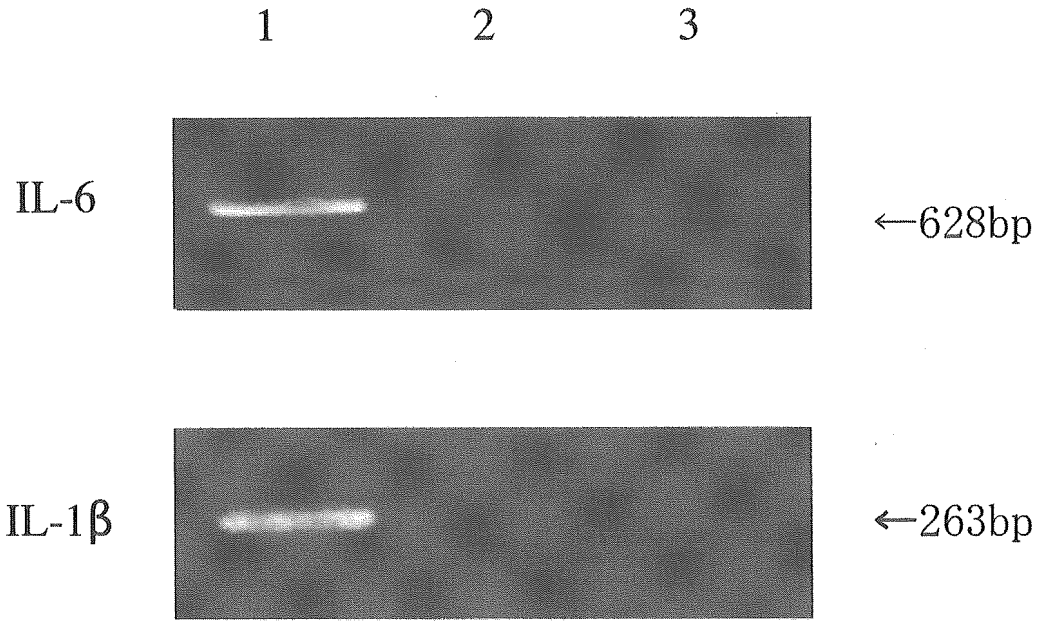

FIG. 3. Results of an RT-PCR assay showing high levels of IL-6 and IL-1β mRNA expression. The RT-PCR products were analyzed on a 2% agarose gel and detected using ethidium bromide staining. Lane 1 = RT positive; Lane 2 = RT negative; Lane 3 = water.

dominant. The IgE production requires cytokines, in particular IL-4, and some investigations have revealed an obligatory role of endogenous IL-6 in IL-4–dependent human IgE synthesis.[25] A balance between Th1 and Th2 is also considered to be critical in the regulation of IgE synthesis.[15] In this case, the overexpression of IL-6 mRNA as Th2 cytokine was confirmed compared with that of IFNλ as the Th1 cytokine, but IL-4 expression could not be demonstrated. It is not possible to draw a definitive conclusion about the dominant levels of IgE in this patient, and a cytokine class switch from Th1 to Th2 profiles, controlled by a variety of environmental or genetic factors, may be associated with an elevated level of IgE. Furthermore, IL-6 may act on B lymphocytes and accelerate the production of IgE as well as IgG.

More recently, VEGF has also been considered to be involved in the pathogenesis of this disease, especially in the marked vascular proliferation of lymph nodes in the interfollicular space.[21] Vascular endothelial growth factor is a specific mitogen for vascular endothelial cells; it therefore has a central role in angiogenesis and can also accelerate the permeability of the vessels.[11] Moreover, its expression is considered to be induced by IL-6.[4] The results of our cytokine study, performed using RT-PCR and immunohistochemical analysis for VEGF, indicate that VEGF-accelerated vasopermeability induced by IL-6 may play a role, at least in part, in lymphoplasmacyte infiltration, which is one of the histopathological characteristics of a chordoid meningioma, although the mechanism for dominancy of T- or B-lymphocytes within the tumor remains unclear.

Conclusions

Chordoid meningioma must be included in the preoperative differential diagnosis of central nervous system neoplasms featuring anemia, hypergammmaglobulinemia, fever of unknown origin, or other systemic illnesses. The clinical outcome of a chordoid meningioma featuring Castleman syndrome is favorable following surgical removal of the tumor, as reported previously. The pathogenesis of Castleman syndrome in the case of chordoid meningioma remains unclear, but a complex cytokine network including IL-6, IL-1β, and VEGF may contribute to the clinicopathological features of chordoid meningioma when associated with this disease.

Acknowledgment

We thank Dr. Y. Nakazato, Department of Pathology, Gunma University Graduate School of Medical Sciences (Maebashi, Japan) for help in the pathological diagnosis.

References

1. Caner H, Acikgoz B, Ozgen T, Colak A, Onol B: Meningiomas of the lateral ventricle. Report on six cases. **Neurosurg Rev 15:** 303–306, 1992
2. Castleman B, Iverson L, Menendez VP: Localized mediastinal lymphnode hyperplasia resembling thymoma. **Cancer 9:** 822–830, 1956
3. Civit T, Taillandier L, Baylac F: Chordoid meningioma. **J Neurosurg 89:**686–687, 1998
4. Cohen T, Nahari D, Cerem LW, Neufeld C, Levi BZ: Interleukin 6 induces the expression of vascular endothelial growth factor. **J Bio Chem 271:**736–741, 1996
5. Couce ME, Aker FV, Scheithauer BW: Chordoid meningioma: a clinicopathologic study of 42 cases. **Am J Surg Pathol 24:** 899–905, 2000
6. Cushing H, Eisenhardt L: **Meningiomas. Their Classification, Regional Behavior, Life History and Surgical End Results.** Springfield, IL: Thomas, 1938
7. Dunn J, Kernahan JW: Observation on the origin of meningioma from the choroid plexus of the lateral ventricle. **Mayo Clin Proc 31:**25–30, 1956

8. Gherardi RK, Bélec L, Fromont G, Divine M, Malapert D, Gaulard P, et al: Elevated levels of interleukin-1 β (IL-1 β) and IL-6 in serum and increased production of IL-1 β mRNA in lymph nodes of patients with polyneuropathy, organomegaly, endocrinopathy, M protein, and skin changes (POEMS) syndrome. **Blood 83:**2587–2593, 1994
9. Guidetti B, Delfini R, Gagliardi FM, Vagnozzi R: Meningiomas of the lateral ventricles. Clinical, neuroradiologic, and surgical considerations in 19 cases. **Surg Neurol 24:**364–370, 1985
10. Ishida F, Kitano K, Kobayashi H, Saito H, Kiyosawa K: Elevated IgG4 levels in a case with multicentric Castleman's disease. **Br J Haematol 99:**981–982, 1997
11. Kalkanis SN, Carroll RS, Zhang J, Zamani AA, Black PM: Correlation of vascular endothelial growth factor messenger RNA expression with peritumoral vasogenic cerebral edema in meningiomas. **J Neurosurg 85:**1095–1101, 1996
12. Kepes JJ, Chen WY, Connors MH, Vogel FS: "Chordoid" meningeal tumors in young individuals with peritumoral lymphoplasmacellular infiltrates causing manifestations of the Castleman syndrome. A report of seven cases. **Cancer 62:**391–406, 1988
13. Kleihues P, Burger PC, Scheithauer BW (eds): **Histological Typing of Tumors of Central Nervous Sysem.** New York: Springer-Verlag, 1993
14. Kobata H, Kondo A, Iwasaki K, Kusaka H, Ito H, Sawada S: Chordoid meningioma in a child. Case report. **J Neurosurg 88:** 319–323, 1998
15. Kurasawa K, Iwamoto I: [Mechanism and regulation of IgE production in allergy. **Nippon Rinsho 54:**434–439, 1996 (Jpn)
16. Lee DK, Kim DG, Choe G, Chi JG, Jung HW: Chordoid meningioma with polyclonal gammopathy. Case report. **J Neurosurg 94:** 122–126, 2001
17. Levy EI, Paino JE, Sarin PS, Goldstein AL, Caputy AJ, Wright DC, et al: Enzyme-linked immunosorbent assay quantification of cytokine concentrations in human meningiomas. **Neurosurgery 39:**823–829, 1996
18. Morimoto A, Sakata Y, Watanabe T, Murakami N: Characteristics of fever and acute-phase response induced in rabbits by IL-1 and TNF. **Am J Physiol 256:**R35-R41, 1989
19. Nakamura M, Roser F, Bundschuh O, Vorkapic P, Samii M: Intraventricular meningiomas; a review of 16 cases with reference to the literature. **Surg Neurol 59:**491–504, 2003
20. Netea MG, Kullberg BJ, Van Der Meer JW: Do only circulating pyrogenic cytokines act as mediators in the febrile response? A hypothesis. **Eur J Clin Invest 29:**351–356, 1999
21. Nishi J, Arimura K, Utsunomiya A, Yonezawa S, Kawakami K, Maeno N, et al: Expression of vascular endothelial growth factor in sera and lymph node of the plasma cell type of Castleman's disease. **Br J Haematol 104:**482–485, 1999
22. Rittierodt M, Tschernig T, Samii M, Walter GF, Stan AC: Evidence of recurrent atypical meningioma with rhabdoid transformation and expression of pyrogenic cytokines in a child presenting with a marked acute-phase response: case report and review of the literature. **J Neuroimmunol 120:**129–137, 2001
23. Rohringer M, Sutherland GR, Louw DF, Sima AA: Incidence and clinicopathological features of meningioma. **J Neurosurg 71:** 665–672, 1989
24. Shaw A: Fibrous tumor in the lateral ventricle of the brain, boney deposits in the arachnoid membrane of the right hemisphere. **Trans Path Soc Lond 5:**18–21, 1854
25. Vercelli D, Jabara HH, Arai K, Yokota K, Geha RS: Endogenous interleukin 6 plays an obligatory role in interleukin 4-dependent human IgE synthesis. **Eur J Immunol 19:**1419–1424, 1989
26. Winter SS, Howard TA, Ritchey AK, Keller FG, Ware RE: Elevated levels of tumor necrosis factor-beta, gamma-interferon, and IL-6 mRNA in Castleman's disease. **Med Pediatr Oncol 26:** 48–53, 1996
27. Yoshizaki K, Matsuda T, Nishimoto N, Kuritani T, Taeho L, Aozasa K, et al: Pathogenic significance of interleukin-6 (IL-6/BSF-2) in Castleman's disease. **Blood 74:**1360–1367, 1989

Manuscript received March 26, 2004.

Address reprint requests to: Toshihiko Wakabayashi, M.D., Center of Genetic and Regenerative Medicine, Nagoya University Hospital 65, Turumai-cho, Showa-ku, Nagoya 466-8550, Japan. email: wakabat@med.nagoya-u.ac.jp.

IFN-β Down-Regulates the Expression of DNA Repair Gene *MGMT* and Sensitizes Resistant Glioma Cells to Temozolomide

Atsushi Natsume,[1] Dai Ishii,[2] Toshihiko Wakabayashi,[1] Takaya Tsuno,[2] Hisashi Hatano,[2] Masaaki Mizuno,[3] and Jun Yoshida[1,2]

[1]Center for Genetic and Regenerative Medicine, Nagoya University Hospital; [2]Department of Neurosurgery, Nagoya University School of Medicine; and [3]Department of Molecular Neurosurgery, Nagoya University Graduate School of Medicine, Nagoya, Japan

Abstract

Alkylating agents, such as temozolomide, are among the most effective cytotoxic agents used for malignant gliomas, but responses remain very poor. The DNA repair protein O^6-methylguanine-DNA methyltransferase (MGMT) plays an important role in cellular resistance to alkylating agents. IFN-β can act as a drug sensitizer, enhancing toxicity against a variety of neoplasias, and is widely used in combination with other antitumor agents such as nitrosoureas. Here, we show that IFN-β sensitizes glioma cells that harbor the unmethylated MGMT promoter and are resistant to temozolomide. By means of oligonucleotide microarray and RNA interference, we reveal that the sensitizing effect of IFN-β was possibly due to attenuation of MGMT expression via induction of the protein p53. Our study suggests that clinical efficacy of temozolomide might be improved by combination with IFN-β using appropriate doses and schedules of administration. (Cancer Res 2005; 65(17): 7573-9)

Introduction

Gliomas are the most common primary tumors of the central nervous system; they account for 30% of adult primary brain tumors. The prognosis for patients with the advanced glioma, glioblastoma multiforme, is very poor; the mean survival period is 8 to 10 months (1). Alkylating agents are among the most effective cytotoxic agents used for treating malignant gliomas, including glioblastoma multiforme, but responses remain very poor. The most frequent site of alkylation in DNA is the O^6 position of guanine, which forms cross-links between adjacent strands of DNA, leading to cell death. A cellular DNA-repair protein, namely O^6-methylguanine-DNA methyltransferase (MGMT) protein, reverses alkylation at the O^6 position of guanine, thereby inhibiting the lethal cross-linking and bringing about resistance to alkylating agents (2, 3). A number of studies have suggested that MGMT deficiency is closely related to the sensitivity of brain tumors to alkylating agents (4–6). Furthermore, because MGMT protein loss may be a result of promoter hypermethylation, it was reported that methylation of the MGMT promoter in gliomas is a useful predictor of the responsiveness to alkylating agents (7). Temozolomide is a novel alkylating agent that has been currently approved for use in treatment of anaplastic astrocytoma in Europe and the United States. A phase II clinical trial has been organized in Japan. This drug is of significance because it can be administered orally; it readily crosses the blood-brain barrier and has minimal side effects (8). Before considering the treatment of malignant gliomas with temozolomide, a major obstacle may be the resistance pathway that occurs due to the actions of MGMT. Hence, efficient attenuation of the function of MGMT, which is expressed in ~70% of gliomas (9), either by direct interaction with protein or by indirect means such as the transcriptional control, is required. It could be advantageous if MGMT depletion can be accomplished by a drug that also has antitumor activity, and, therefore, synergistic effects with the alkylating agent may occur. Type I IFNs, including IFN-α and IFN-β, a family of cytokines that elicit pleiotropic biological effects, are widely used either alone or in combination with other antitumor agents such as nitrosoureas in the treatment of malignant gliomas. Among the multiple functions of type I IFNs against human neoplasias, type I IFNs, particularly IFN-β, can act as a drug sensitizer enhancing toxicity against a variety of neoplasias when given in combination with nitrosoureas (10). Therefore, it is of interest to examine whether IFN-β can enhance chemosensitivity of malignant gliomas against temozolomide, the new alkylkating agent; to evaluate the mechanism; and to provide an experimental basis for the rational clinical use of such combinations.

Materials and Methods

Cell lines and reagents. Human glioma cell lines (T98, AO2, SKMG1, U251nu/nu, U251SP, and U251MG) derived from the Memorial Sloan-Kettering Cancer Institute (New York, NY) were maintained at 37°C in a humidified atmosphere of 5% CO_2 in air in Eagle's medium (Nissui, Tokyo, Japan). Medium was supplemented with 10% fetal bovine serum (FBS), 5 mmol/L L-glutamine, 2 mmol/L nonessential amino acids, and antibiotics (100 units/mL penicillin and 100 μg/mL streptomycin). Human IFN-β and temozolomide were kindly supplied by Toray, Co., Ltd. (Kamakura, Japan), and the Schering-Plough Research Institute (Kenilworth, NJ), respectively. Temozolomide readily discomposes in aqueous solution into DMSO.

RNA interference experiments. The target sequence in p53 and the control nonsilencing sequence are CGGCAUGAACCGGAGGCCCAU and AATTCTCCGAACGTGTCACGT, respectively. These synthetic sense and antisense oligonucleotides were obtained from Qiagen (Hilden, Germany). For the annealing of small interfering RNA (siRNA) oligonucleotides, sense and antisense oligonucleotides were incubated in siRNA Suspension Buffer (Qiagen) for 1 minute at 90°C, followed by 60 minutes at 37°C. siRNA oligonucleotides were mixed with Oligofectamine reagent (Invitrogen, Carlsbad, CA) in Opti-MEM (Life Technologies, Gaithersburg, MD). Cultured cells were washed with medium without serum and added to the siRNA-Oligofectamine mixture, of which the final concentration was 200 nmol/L. Medium with 10% FBS was added 4 hours later.

Determination of cell growth. To compare chemosensitivity of glioma cell lines to temozolomide, the agent (final concentration of 0-1,000 μmol/L) was added to the culture medium at 24 hours after aliquots of 2×10^4 cells/well were placed in triplicate wells. Incubation was continued for 72 hours, and the number of viable cells was counted by trypan blue exclusion method. The number was expressed as a percentage of untreated control. The statistical significance of difference was determined by ANOVA using

Requests for reprints: Atsushi Natsume, Department of Neurosurgery, Nagoya University School of Medicine, 65 Tsurumai-cho, Showa-ku, 4668550 Nagoya, Aichi, Japan. Phone: 81-52-744-2353; Fax: 81-52-744-2360; E-mail: anatsume@med.nagoya-u.ac.jp.
©2005 American Association for Cancer Research.
doi:10.1158/0008-5472.CAN-05-0036

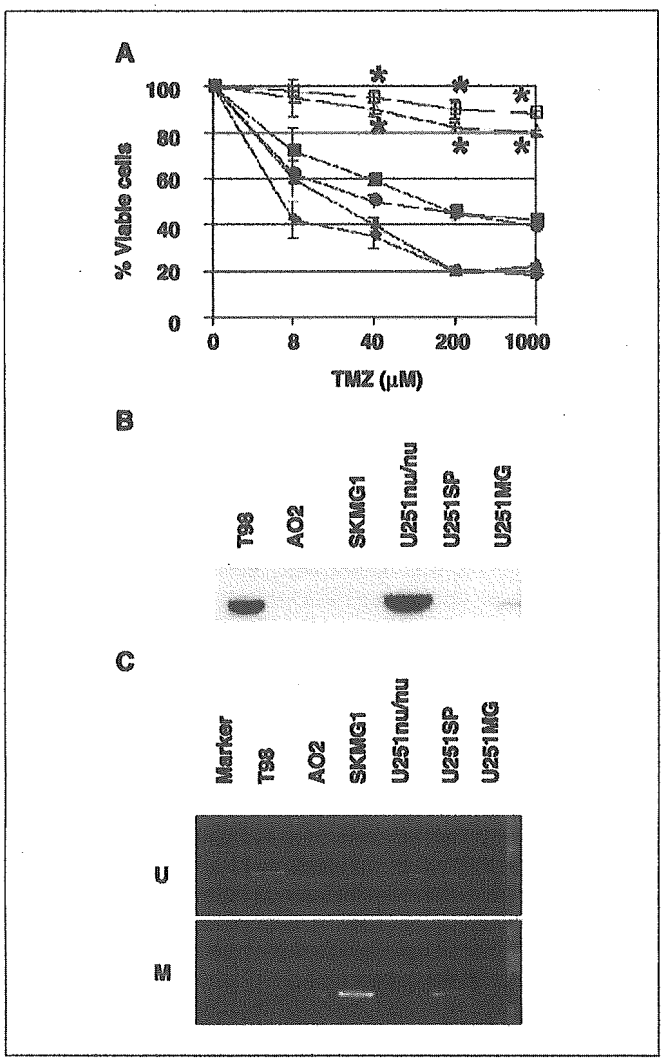

Figure 1. Comparisons among human glioma cell lines. *A*, the antitumor effects of temozolomide against six human glioma cell lines: T98 (□), AO2 (▲), SKMG1 (●), U251nu/nu (△), U251SP (■), and U251MG (◆). At 72 hours after temozolomide (final concentration of 0-1,000 μmol/L) was added to the culture medium, the number of viable cells was counted. The number was expressed as a percentage of untreated control. $^*P < 0.05$ versus AO2, SKMG1, U251SP, and U251MG at each dose. *B*, Western blot analysis of MGMT in human glioma cell lines. The cell lysate was subjected to Western blotting with anti-MGMT antibody. *C*, methylation-specific PCR analysis of human glioma cell lines. *U* and *M*, reactions for unmethylated and methylated sequences, respectively.

Bonferroni's correction for the multiple comparisons used. For sensitizing assay of IFN-β to temozolomide, IFN-β (100 IU/mL) and temozolomide (100 μmol/L) were added at 24 and 48 hours after cell inoculation, respectively. The number of viable cells was counted at 96 hours. To examine the effect of siRNA for p53 on the growth of T98 cells treated with IFN-β and temozolomide, either siRNA for p53 or nonsilencing siRNA was transfected as described above at 24 hours after aliquots of 4×10^4 cells/well were placed in triplicate wells. IFN-β (100 IU/mL) and temozolomide (100 μmol/L) were added at 28 and 48 hours, respectively. The number of viable cells was counted at 96 hours.

Western blot analysis. Cell lysis and immunoblotting were carried out as described (11). Antibodies against the following proteins were purchased: p53 (DO-1: Santa Cruz Biotechnology, Santa Cruz, CA), p21 (EA10: Oncogene Research Products, San Diego CA), MGMT (MT3.1: Neomarkers, Fremont, CA), and β-actin (AC-15: Sigma-Aldrich, St. Louis, MO). Band intensities were quantified by densitometric scanning using the NIH IMAGE program.

Genomic DNA extraction and methylation-specific PCR. Genomic DNA was extracted using the QIAmp DNA Mini kit (Qiagen) following the manufacturer's instructions. DNA methylation patterns in the promoter region of the *MGMT* gene (Genbank accession no. X_61657) were determined by methylation-specific PCR as previously described (12). Primers for either methylated or unmethylated alleles were 5′-TTTCGACGTT-CGTAGGTTTTCGC-3′ (sense) and 5′-GCACTCTTCCGAAAACGAAACG-3′ (antisense) or 5′-TTTGTGTTTTGATGTTTGTAGGTTTTTGT-3′ (sense) and

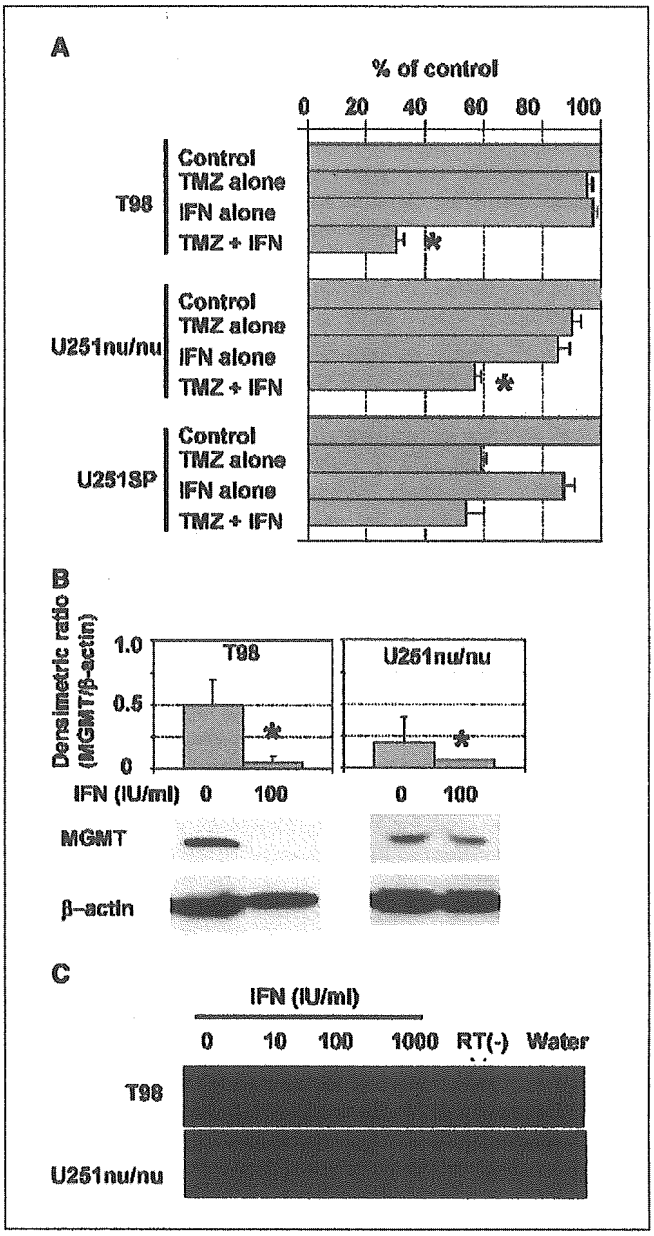

Figure 2. IFN-β sensitizes T98 and U251nu/nu glioma cells to temozolomide and down-regulated MGMT expression. *A*, IFN-β sensitizes the resistant T98 and U251nu/nu cell lines, but not the sensitive U251SP cell line, to temozolomide. The cells were incubated in a culture medium containing IFN-β (100 IU/mL) for 24 hours before the addition of temozolomide (final concentration of 100 μmol/L). Seventy-two hours after, the number of viable cells was counted and expressed as a percentage of untreated control ($^*P < 0.05$). *B*, Western blot analysis of MGMT in T98 and U251nu/nu cells treated with IFN-β. Western blotting was done as in Fig. 1*B*. The histogram shows the amount of MGMT relative to that of β-actin. *Columns*, mean from three independent experiments; *bars*, SD ($^*P < 0.05$). *C*, RT-PCR analysis for MGMT mRNA. No reverse-transcription control (*RT*−) is also shown.

Table 1.

A. Increase in gene expression in T98 cells by IFN-β

Symbol	Genes	Genbank accession no.	Mean
RBP2	*Retinoblastoma-binding protein 2*	S66431.1	2.012
PKB	*Protein kinase B*	X61037.1	2.024
FGF-9	*Fibroblast growth factor 9*	D14838.1	2.035
Grb14	*Grb14*	L76687.1	2.035
VCAM-1	*Vascular cell adhesion molecule 1 (VCAM-1)*	X53051.1	2.035
IL18	*Interleukin 18 (IFN-γ–inducing factor)*	NM_001562.2	2.047
HOX-11	*Homeobox protein (HOX-11)*	M75952.1	2.055
bcl-w	*Gi|1572492|gb|U59747.1|HSU59747 Human Bcl-w (bcl-w) mRNA, complete cds*	U59747.1	2.074
IGFBP-5	*Insulin-like growth factor binding protein 5*	M62782.1	2.081
Clk2	*Clk2*	L29216.1	2.098
NIK	*Serine/threonine protein kinase*	Y10256.1	2.106
p68K	*p68 kinase*	M35663.1	2.112
IGF-II	*Human insulin–like growth factor II*	M29645.1	2.121
GALNAC4S-6ST	*B-cell RAG-associated protein*	NM_014863.1	2.128
FGF-10	*FGF-10*	AB002097.1	2.129
FRA-2	*Human fra-2*	X16706.1	2.134
FASL	*Fas ligand*	D38122.1	2.146
PDGF	*Platelet-derived growth factor A-chain*	A09204.1	2.158
E1A-F	*E1A-F*	D12765.1	2.163
c-myc	*c-myc*	D89667.1	2.167
hTRIP	*hTRIP (hTRIP)*	U77845.1	2.185
CALM2	*Calmodulin 2 (phosphorylase kinase, δ)*	NM_001743.3	2.207
PUMP-1	*PUMP-1 gene encoding PUMP*	Z11887.1	2.207
Bcl2	*Bcl2, p53-binding protein Bbp/53BP2 (BBP/53BP2)*	U58334.1	2.207
MKK6	*MAP kinase kinase 6*	U39657.1	2.218
JNK3A1	*NK3 α1 protein kinase*	U34820.1	2.242
pS2	*pS2 mRNA induced by estrogen from human breast cancer cell line MCF-7*	X00474.1	2.273
ICAM-2	*ICAM-2, cell adhesion ligand for LFA-1*	X15606.1	2.276
CREM	*Cyclic AMP-responsive element modulator (CREM)*	S68271.1	2.289
Humig	*Humig*	X72755.1	2.289
NFAT1	*Transcription factor NFAT1 isoform C (NFAT1)*	U43342.1	2.289
SFPQ	*Splicing factor proline/glutamine–rich (polypyrimidine tract binding protein associated; SFPQ)*	NM_005066.1	2.302
N-CoR	*Nuclear receptor corepressor*	AF044209.1	2.333
IGFBP3	*Growth factor-binding protein-3 precursor (IGFBP3)*	M35878.1	2.359
IRF-1	*IFN regulatory factor 1*	X14454.1	2.4
IL-11R	*Interleukin-11 receptor*	Z38102.1	2.417
hsp70	*Heat shock protein 70 (hsp70)*	L12723.1	2.424
bcl-3	*B-cell lymphoma 3-encoded protein (bcl-3)*	M31732.1	2.441
FAS/Apo 1	*FAS/Apo 1 mRNA for FAS soluble protein (clone FAS Exo4Del)*	Z70519.1	2.471
HSP75	*Homo sapiens mitochondrial HSP75*	L15189.1	2.481
ICE-LAP6	*Cysteine protease ICE-LAP6*	U56390.1	2.485
G0S8	*Helix-loop-helix basic phosphoprotein*	L13463.1	2.487
HEK2	*HEK2 mRNA for protein tyrosine kinase receptor*	X75208.1	2.493
ERK2	*40 kDa protein kinase related to rat ERK2*	Z11695.1	2.503
KIAA0347	*KIAA0347*	AB002345.2	2.504
APAF1	*Apoptotic protease–activating factor (APAF1), transcript variant 2*	NM_001160.2	2.513
TRA1	*Tumor rejection antigen (gp96) 1*	NM_003299.1	2.574
TNF	*Tumor necrosis factor superfamily member LIGHT*	AF036581.1	2.582
FGF-5	*Fibroblast growth factor-5 (FGF-5)*	M37825.1	2.616
PPAR	*Peroxisome proliferator–activated receptor*	L02932.1	2.616
TIPM3	*Tissue inhibitor of metalloproteinases-3*	U14394.1	2.628
Mch3	*Mch3 isoform α(Mch3)*	U37448.1	2.698
PTPRZ	*Protein tyrosine phosphatase ζ-polypeptide (PTPRZ)*	M93426.1	2.698
RPGR	*Retinitis pigmentosa GTPase regulator (RPGR)*	NM_000328.1	2.741
ENO3	*Enolase 3, (β, muscle; ENO3), transcript variant 1*	NM_001976.2	2.754

(*Continued on the following page*)

Table 1. (Cont'd)

A. Increase in gene expression in T98 cells by IFN-β

Symbol	Genes	Genbank accession no.	Mean
NFKB1	*Nuclear factor of kappa light polypeptide gene enhancer in B-cells 1 (p105; NFKB1)*	NM_003998.2	2.761
HRK	*Activator of apoptosis Hrk (HRK)*	U76376.1	2.774
IFITM3	*IFN-induced transmembrane protein 3 (1-8U; IFITM3)*	NM_021034.1	2.882
IL15RA	*Interleukin-15 receptor αchain precursor (IL15RA)*	U31628.1	2.918
AMPD2	*AMP deaminase 2 (isoform L; AMPD2)*	NM_004037.5	2.989
DNAJA1	*DnaJ (Hsp40) homologue, subfamily A, member 1*	NM_001539.1	3.184
HLA-C	*MHC class I HLA-C allele HLA-4*	M11886.1	3.265
IFN-γ	*IFN-γ*	X13274.1	3.27
p53	*p53 cellular tumor antigen*	M14694.1	3.301
HLA-B	*MHC, class I*	NM_005514.4	3.374
CHED	*cdc2-related protein kinase*	M80629.1	3.686
GADD45	*Gadd45*	S40706.1	3.694
BPAG1	*Bullous pemphigoid antigen 1, 230/240kDa (BPAG1), transcript variant 1e, mRNA*	NM_001723.3	3.793
ISGF-3	*Transcription factor ISGF-3*	M97936.1	3.938
TGFR	*Transforming growth factor-βtype III receptor*	L07594.1	4.341
MC4R	*Melanocortin 4 receptor*	NM_005912.1	10.821

B. Decrease in gene expression in T98 cells by IFN-β

DR3	*Death receptor 3 (DR3)*	U72763.1	0.5
GST-pi-1	*Anionic glutathione-S-transferase (GST-pi-1)*	X15480.1	0.5
TSHR	*Thyroid stimulatory hormone receptor*	M32215.1	0.5
PRDX6	*Peroxiredoxin 6*	NM_004905.2	0.499
IGFBP6	*Insulin-like growth factor binding protein 6*	M62402.1	0.499
HRR-1	*Farnesol receptor*	U68233.1	0.498
IL8RBA	*Interleukin-8 receptor type A*	U11870.1	0.497
RPS2	*Ribosomal protein S2*	NM_002952.2	0.493
COX6C	*Cytochrome coxidase subunit Vic*	NM_004374.2	0.49
HINT1	*Histidine triad nucleotide–binding protein 1*	NM_005340.2	0.489
E2F-1	*pRB-binding protein*	M96577.1	0.483
SKP1A	*S-phase kinase–associated protein 1A (p19A; SKP1A), transcript variant 1*	NM_006930.2	0.483
HS1	*HS1 protein*	X57347.1	0.478
PPP2CA	*Protein phosphatase 2 (formerly 2A), catalytic subunit, αisoform*	NM_002715.1	0.478
G3PD	*Glyceraldehyde-3-phosphate dehydrogenase*	X01677.1	0.473
VitDR	*Vitamin D receptor*	J03258.1	0.472
SEC61B	*Sec61 βsubunit*	NM_006808.2	0.47
SHC	*SHC*	X68148.1	0.47
COX6A1	*Cytochrome coxidase subunit VIa polypeptide 1*	NM_004373.2	0.46
PIN1	*Peptidyl-prolyl isomerase and essential mitotic regulator*	U49070.1	0.457
IL5Rα	*Interleukin 5 receptor α*	M75914.1	0.443
RAB	*Cellular cofactor*	L42025.1	0.435
CD6	*T-cell glycoprotein CD6*	X60992.1	0.434
NDUFB3	*NADH dehydrogenase (ubiquinone) 1 βsubcomplex, 3, 12 kDa*	NM_002491.1	0.433
TXN	*Thioredoxin*	NM_003329.1	0.431
COX4I1	*Cytochrome coxidase subunit IV isoform 1*	NM_001861.2	0.426
SMRT	*Silencing mediator of retinoid and thyroid hormone action*	U37146.1	0.423
ERK3	*ERK3*	X80692.1	0.422
TCRB	*T-cell receptor βchain*	L07294.1	0.421
LGALS1	*Lectin, galactoside-binding, soluble, 1 (galectin 1)*	NM_002305.2	0.417
SOD1	*Superoxide dismutase 1*	NM_000454.2	0.414
ROX	*ROX protein*	X96401.1	0.41
BAG1	*BCL2-associated athanogene*	NM_004323.2	0.409
DC50	*Hypothetical protein DC50*	NM_031210.3	0.407
FTH1	*Ferritin, heavy polypeptide 1*	NM_002032.1	0.398
XRCC5	*X-ray repair complementing defective repair in Chinese hamster cells 5*	NM_021141.2	0.387

(*Continued on the following page*)

Table 1. (Cont'd)

B. Decrease in gene expression in T98 cells by IFN-β

Symbol	Genes	Genbank accession no.	Mean
GSTO1	*Glutathione S-transferase ω1*	NM_004832.1	0.384
TPM2	*Tropomyosin 2 (β)*	NM_003289.1	0.377
CD27L	*CD27 ligand*	L08096.1	0.374
PRDX1	*Peroxiredoxin 1*	NM_002574.2	0.372
MAD-3	*MAD-3 mRNA encoding IkB-like activity*	M69043.1	0.369
CRAF1	*CD40 receptor associated factor 1*	U21092.1	0.365
KIP2	*Cdk-inhibitor p57KIP2*	U22398.1	0.362
RPLP1	*Ribosomal protein, large, P1*	NM_001003.2	0.356
PIG3	*Pig3*	AF010309.1	0.341
GAS	*Growth-arrest-specific protein*	L13720.1	0.33
TMSB10	*Thymosin, β10 (TMSB10)*	NM_021103.2	0.322
ME491	*Melanoma-associated antigen ME491*	X07982.1	0.313
ANXA2	*Annexin A2*	NM_004039.1	0.29
CollagenaseV	*Collagenase type IV*	J03210.1	0.29
S100A2	*S100 calcium-binding protein A2*	NM_005978.2	0.281
calpain	*Calcium-activated neutral protease large subunit*	X04366.1	0.262
FTL	*Ferritin, light polypeptide*	NM_000146.2	0.239

NOTE: p53-related genes are in bold. The mean was based on three replicate arrays analyzed statistically as described in the text.

5′-AACTCCACACACTCTTCCAAAAACAAAACA-3′ (antisense). All PCRs were done with positive controls for methylated alleles and no DNA control. Human placental DNA was treated *in vitro* with excess SssI methyltransferase (New England Biolabs, Beverly, MA), generating DNA completely methylated at CpG sites, served as the positive control for methylated MGMT, and then the PCR conditions were determined. Each PCR product was loaded onto a 3% agarose gel, stained with ethidium bromide, and visualized under UV illumination.

Reverse transcriptase-PCR. To investigate MGMT mRNA expression, reverse transcription-PCR (RT-PCR) was done using the Superscript first-strand synthesis system for RT-PCR (Invitrogen) as previously described (13). β-actin–specific PCR products from the same RNA samples were amplified and served as internal controls.

Microarray analysis. T98 cells were incubated with 100 IU/mL of IFN-β for 48 hours, and RNA was isolated. Standard Trizol preparation protocol (Invitrogen) and reagents were used for total RNA isolation. RNA amplification and labeling were done using the Amino Allyl MessageAmp aRNA kit (Ambion, Austin, TX). Briefly, after reverse transcription reactions (2 μg total RNA/sample) were preformed, double-stranded cDNA was transcribed *in vitro* into amino allyl cRNA. The purified and concentrated cRNA (5 μg) was coupled with either Cy3 or Cy5 dyes (Amersham Biosciences). The dye-labeled aRNA was purified from uncoupled dye using Micro Bio-Spin P-30 Tris chromatography columns (Bio-Rad, Hercules, CA) and MicroconYM-30 centrifugal filter devices (Millipore, Billerica, MA). The cRNA was fragmented in fragmentation buffer [40 mmol/L Tris-acetate (pH 8.1), 100 mmol/L potassium acetate, 30 mmol/L magnesium acetate] at 94°C for 15 minutes and purified with Microcon YM-10 (Millipore). Microarrays were preblocked with 1% bovine serum albumin solution. Fragmented cRNA was added to microarrays in hybridization solution and hybridized at 42°C for 16 hours. After this, arrays were washed, scanned at 10 μm pixel size, gridded, and analyzed (GenePix 4000B; Axon Instruments, Union City, CA). Background was subtracted, and the median sum and median ration were calculated. Flagged spots and spots with sum intensity (CH1, CH2) <100 absorbance units were excluded. Data were normalized by trimmed mean at 10% to account for differences in the amounts of RNA labeled or labeling efficiencies.

Chromatin immunoprecipitation assay. The chromatin immunoprecipitation assay was done according to the protocol of the manufacturer (Upstate Biotechnology, Lake Placid, NY) with a slight modification. The specific antibodies used for immunoprecipitations were the anti-p53 antibody and a control antibody. After protein-DNA cross-links in the immunoprecipitates were reversed, the purified DNA was analyzed by PCR (35 cycles; 45 seconds at 95°C, 45 seconds at 55°C, 60 seconds at 72°C) with primers that detect the MGMT promoter sequence [5′-GCTCCAGGGAA-GAGTGTCCTCTGC-TCCCT-3′ (sense) and 5′-GGCCTGTGGTGGGCGAT-GCCGTCCAG-3′ (antisense)] and glyceraldehyde-3-phosphate dehydrogenase (GAPDH) promoter (provided with the kit). The PCR products were visualized on an ethidium bromide gel.

Results and Discussion

Chemosensitivity to temozolomide, MGMT expression, and MGMT promoter hypermethylation of human glioma cell lines. First, we compared chemosensitivity of six human glioma cell lines to temozolomide; T98 and U251nu/nu cell lines were significantly resistant, whereas the other four (AO2, SKMG1, U251SP, and U251MG) showed similar degrees of sensitivity in a dose-dependent manner (Fig. 1*A*). MGMT expression was not detected by Western blot in the sensitive cell lines (Fig. 1*B*), and the hypermethylation of MGMT promoter was as assessed by methylation-specific PCR (Fig. 1*C*), but this was not observed in the T98 and U251nu/nu cell lines. Thus, the results showed that hypermethylation of MGMT promoter could prevent expression of this gene and be associated with chemosensitivity of glioma cells to temozolomide, which was consistent with the results of reported studies (7). Because ~70% of gliomas express MGMT (9), it is essential to suppress the expression or function of MGMT in an efficient manner if treatment with the aid of temozolomide is to be considered.

IFN-β sensitizes resistant glioma cells to temozolomide and down-regulates MGMT expression. IFNs are a family of cytokines

that possess pleiotropic biological effects mediated by a number of responsive genes. IFNs were the first human proteins to be recognized as being effective in cancer therapy (14). Although identified and named for their action to interfere with viral replication, IFNs have immunomodulatory, cell differentiative, antiangiogenic, and antiproliferative effects (15, 16). In the previous studies, we showed that IFN-β has multiple functions relevant to antitumor activity: (*a*) cytostatic effect on glioma cells, (*b*) supportive action on the differentiation of CTLs and augmentation of their antitumor immune responses, and (*c*) behavior as a drug or radiation sensitizer enhancing toxicity against gliomas (10).

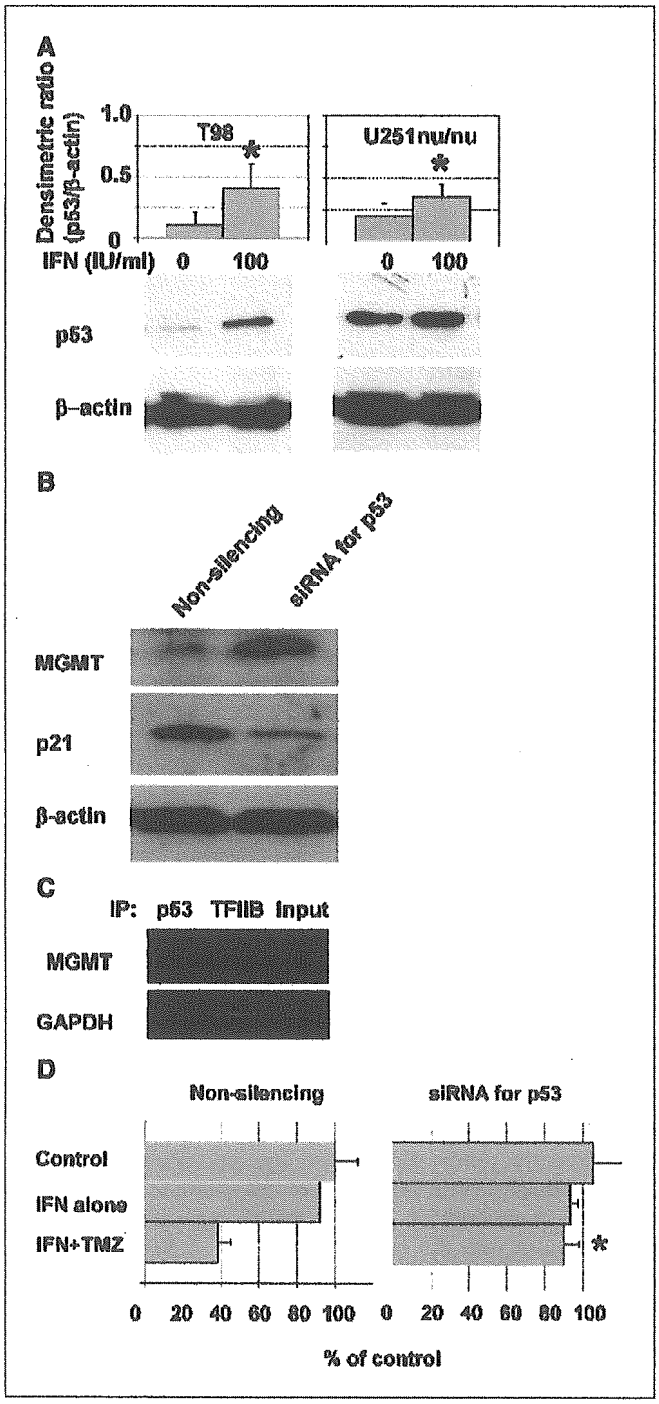

To examine whether IFN-β sensitizes T98 and U251nu/nu cell lines that are resistant to temozolomide, the cells were incubated in a culture medium containing IFN-β (100 IU/mL) for 24 hours before the addition of temozolomide (final concentration of 100 μmol/L). As shown in Fig. 2*A*, whereas IFN-β or temozolomide alone did not suppress cell growth of both T98 and U251nu/nu cells significantly, a combination of IFN-β and temozolomide markedly inhibits the growth. On the other hand, U251SP cell lines that are sensitive to temozolomide, but are resistant to IFN-β did not show the synergistic cytotoxic effect of temozolomide and IFN-β. Consequently, we hypothesized that IFN-β might enhance chemosensitivity due to reduction of MGMT expression and did Western blotting and RT-PCR for MGMT (Fig. 2*B* and *C*). It was shown that IFN-β decreased both MGMT protein and mRNA levels of both T98 and U251nu/nu cells at 48 hours after treatment. Thus, IFN-β decreases MGMT transcription directly or indirectly and sensitizes resistant glioma cells to temozolomide.

Microarray analysis of IFN-β–regulated genes. Because limited information regarding the transcriptional regulation of IFN-β is available, we introduced microarray technology that enables the simultaneous examination of expression of a large number of genes in an experimental condition. This microarray contains 1,300 functionally well-characterized genes involved in various important cellular processes, including the IFN-related pathway, apoptosis, cell cycle, transcription, and immunology. The microarray experiments were repeated thrice about the T98 cell lines that showed the most drastic change of MGMT expression after IFN-β treatment. Data analysis identified 71 significantly induced genes and 54 repressed genes in several different categories in T98 cells treated with IFN-β compared with the parental cells. The representative results of these comparisons are reported in Table 1. Some of the alterations in gene expression following IFN-β treatment confirm the involvement of pathways known to be active in this process, and this was anticipated from prior evidence. Consistent with a report that the *p53* gene is transcriptionally induced by IFN-β through ISGF3 activation (11), our microarray data showed that the *p53* gene and its downstream genes, including *bcl-2*, *FAS/Apo1*, and *Gadd45*, are up-regulated in glioma cells treated with IFN-β, suggesting that *p53* induction may be a key involved in antitumor action of IFN-β. Thus, we focused on IFN-β–mediated *p53* induction. By Western blot, we confirmed that *p53* expression level in both T98 cells treated with IFN-β was markedly higher than that in the

Figure 3. IFN-β down-regulates MGMT expression via induction of p53. *A*, up-regulation of the protein p53 in T98 and U251nu/nu cells by IFN-β. The cell lysate of cells treated with IFN-β (100 IU/mL) was subjected to Western blotting with anti-p53 and anti–β-actin antibodies. The histogram shows the amount of p53 relative to that of β-actin. *Columns*, mean values from three independent experiments; *bars*, SD (* $P < 0.05$). *B*, RNA interference experiments for p53. After p53 was knocked down by the siRNA specific for p53, Western blotting for MGMT, p21, and β-actin was done. The siRNA with nonsilencing sequence was used as a control. The specific knockdown was confirmed by the diminished expression level of p21, a well-known target gene of *p53*. *C*, chromatin immunoprecipitation assay. The protein p53 binding to the MGMT promoter element was examined. *Lane 1*, PCR amplification of MGMT and GAPDH sequences in immunoprecipitated chromatin fragments with anti-p53 antibody. *Lane 2*, result of PCR using immunoprecipitated samples with control antibody against TFIIB, the known transcriptional factor of GAPDH. *Lane 3*, PCR amplification of the total input DNA. *D*, cancellation of the sensitizing effect of IFN-β by p53 siRNA. T98 cells were treated with the siRNA for p53 or the nonsilencing siRNA before the treatments of IFN-β (100 IU/mL) and temozolomide (100 μmol/L). Seventy-two hours after, the number of viable cells was counted. *$P < 0.05$ versus the treatment group with nonsilencing siRNA, IFN-β, and temozolomide.

untreated cells and the similar phenomenon was observed in the U251nu/nu cells as well (Fig. 3*A*).

IFN-β down-regulates MGMT expression via protein p53. For >10 years, p53 has been the focus of intensive research. This has led to a plethora of information regarding p53, its biological roles, and its relevance to cancer (17). p53 is primarily a sequence-specific transcriptional activator. It binds to cognate p53-responsive elements within the genome and activates the transcription of genes residing in the vicinity of these binding sites. The proteins encoded by the p53 target genes, whose number is probably in the hundreds, contribute in multiple ways to the biological effects of p53. The biological outcomes of p53 activity include apoptosis, inhibition of cell cycle progression, senescence, differentiation, and accelerated DNA repair. We first confirmed that siRNA for p53 specifically knocked down the protein p53 function by examining the diminished expression level of *p21*, a well-known target gene of p53 (Fig. 3*B*). As shown in Fig. 3*B*, knockdown of p53 by siRNA increased MGMT expression in T98 cells. Therefore, p53 can down-regulate transcription of MGMT. To further investigate whether protein p53 directly interacts with MGMT promoter and down-regulates transcription of MGMT, we carried out chromatin immunoprecipitation assay. We observed that MGMT promoter, but not GAPDH promoter, coprecipitated with p53. The irrelevant antibody specific to TFIIB, which is a transcription factor of GAPDH, did not coprecipitate with MGMT promoter (Fig. 3*C*). These findings are in agreement with the previous reports showing that p53 reduces the basal activity of the MGMT promoter, and adenoviral vector–mediated overexpression of p53 reduces MGMT expression (18, 19), although some papers suggested that inactivated MGMT may be linked to cytotoxic effect of alkylating agents and cell signaling events, but was independent of p53 status (20). The reasons for these differences are unclear and may be cell type dependent. Moreover, in cell growth experiments, knocking down of p53 before IFN-β treatment nullified the synergistic inhibitory effect of IFN-β and temozolomide on T98 cell growth (Fig. 3*D*). Thus, acting together, IFN-β down-regulates MGMT transcription via induction of the p53 expression and sensitizes resistant glioma cells to temozolomide. In conclusion, this report shows that IFN-β is able to decrease MGMT levels in glioma cells via the inhibition of *MGMT* gene transcription. Moreover, pretreatment of glioma cells with IFN-β markedly enhances chemosensitivity to temozolomide. This suggests that clinical efficacy of temozolomide might be improved by combination with IFN-β using appropriate doses and schedules of administration.

Acknowledgments

Received 1/6/2005; revised 5/7/2005; accepted 6/23/2005.

The costs of publication of this article were defrayed in part by the payment of page charges. This article must therefore be hereby marked *advertisement* in accordance with 18 U.S.C. Section 1734 solely to indicate this fact.

The authors especially thank NGK Insulators, Ltd for making the custom made microarray, and thank Ms. Yasuko Yoshida and Mr. Saichi Yamada (NGK Insulators, Ltd) for technical assistance.

References

1. Fine HA, Dear KB, Loeffler JS, Black PM, Canellos GP. Meta-analysis of radiation therapy with and without adjuvant chemotherapy for malignant gliomas in adults. Cancer 1993;71:2585–97.
2. Ludlum DB. DNA alkylation by the haloethylnitrosoureas: nature of modifications produced and their enzymatic repair or removal. Mutat Res 1990;233:117–26.
3. Pegg AE, Dolan ME, Moschel RC. Structure, function, and inhibition of O^6-alkylguanine-DNA alkyltransferase. Prog Nucleic Acid Res Mol Biol 1995;51:167–223.
4. Jaeckle KA, Eyre HJ, Townsend JJ, et al. Correlation of tumor O^6 methylguanine-DNA methyltransferase levels with survival of malignant astrocytoma patients treated with bis-chloroethylnitrosourea: a Southwest Oncology Group study. J Clin Oncol 1998;16:3310–5.
5. Mineura K, Yanagisawa T, Watanabe K, Kowada M, Yasui N. Human brain tumor $O(6)$-methylguanine-DNA methyltransferase mRNA and its significance as an indicator of selective chloroethylnitrosourea chemotherapy. Int J Cancer 1996;69:420–5.
6. Belanich M, Pastor M, Randall T, et al. Retrospective study of the correlation between the DNA repair protein alkyltransferase and survival of brain tumor patients treated with carmustine. Cancer Res 1996;56:783–8.
7. Esteller M, Garcia-Foncillas J, Andion E, et al. Inactivation of the DNA-repair gene *MGMT* and the clinical response of gliomas to alkylating agents. N Engl J Med 2000;343:1350–4.
8. Stupp R, Gander M, Leyvraz S, Newlands E. Current and future developments in the use of temozolomide for the treatment of brain tumours. Lancet Oncol 2001;2:552–60.
9. Silber JR, Mueller BA, Ewers TG, Berger MS. Comparison of O^6-methylguanine-DNA methyltransferase activity in brain tumors and adjacent normal brain. Cancer Res 1993;53:3416–20.
10. Yoshida J, Kato K, Wakabayashi T, Enomoto H, Kageyama N. Antitumor activity of interferon-β against malignant glioma in combination with chemotherapeutic agent of nitrosourea (ACNU). In: Cantell K, Schellekens H, editors. The Biology of the Interferon Systems. Boston: Martinus Nijhoff; 1986. p. 339–406.
11. Takaoka A, Hayakawa S, Yanai H, et al. Integration of interferon-α/β signalling to p53 responses in tumour suppression and antiviral defence. Nature 2003;424:516–23.
12. Herman JG, Graff JR, Myohanen S, Nelkin BD, Baylin SB. Methylation-specific PCR: a novel PCR assay for methylation status of CpG islands. Proc Natl Acad Sci U S A 1996;93:9821–6.
13. Esteller M, Toyota M, Sanchez-Cespedes M, et al. Inactivation of the DNA repair gene O^6-methylguanine-DNA methyltransferase by promoter hypermethylation is associated with G to A mutations in K-*ras* in colorectal tumorigenesis. Cancer Res 2000;60:2368–71.
14. Chawla-Sarkar M, Lindner DJ, Liu YF, et al. Apoptosis and interferons: role of interferon-stimulated genes as mediators of apoptosis. Apoptosis 2003;8:237–49.
15. Borden EC. WB interferons. 5th ed. Toronto: B.C. Decker, Inc.; 2000. p. 815–24.
16. Stark GR, Kerr IM, Williams BR, Silverman RH, Schreiber RD. How cells respond to interferons. Annu Rev Biochem 1998;67:431–42.
17. Oren M. Decision making by p53: life, death and cancer. Cell Death Differ 2003;10:431–42.
18. Grombacher T, Eichhorn U, Kaina B. p53 is involved in regulation of the DNA repair gene O^6-methylguanine-DNA methyltransferase (MGMT) by DNA damaging agents. Oncogene 1998;17:845–51.
19. Harris LC, Remack JS, Houghton PJ, Brent TP. Wild-type p53 suppresses transcription of the human O^6-*methylguanine-DNA methyltransferase* gene. Cancer Res 1996;56:2029–32.
20. Yan L, Donze JR, Liu L. Inactivated MGMT by O^6-benzylguanine is associated with prolonged G2/M arrest in cancer cells treated with BCNU. Oncogene 2005;24:2175–83.

J Neurosurg (Pediatrics 3) 102:299–302, 2005

Multicentric atypical teratoid/rhabdoid tumors occurring in the eye and fourth ventricle of an infant

Case report

MITSUGU FUJITA, M.D., MIHO SATO, M.D., MAKOTO NAKAMURA, M.D., KAZUKO KUDO, M.D., TETSURO NAGASAKA, M.D., MASAAKI MIZUNO, M.D., EMI AMANO, M.D., YOKO OKAMOTO, M.D., YOSHIHIRO HOTTA, M.D., HISASHI HATANO, M.D., NORIMOTO NAKAHARA, M.D., TOSHIHIKO WAKABAYASHI, M.D., AND JUN YOSHIDA, M.D.

Department of Ophthalmology, Hamamatsu University School of Medicine, Hamamatsu; Departments of Neurosurgery, Ophthalmology, Pediatrics and Developmental Pediatrics, and Molecular Neurosurgery, Nagoya University Graduate School of Medicine; and Division of Pathology, Clinical Laboratory, and Center for Genetic and Regenerative Medicine, Nagoya University Hospital, Nagoya, Japan

✓Atypical teratoid/rhabdoid tumors (AT/RTs) are aggressive malignant tumors found in infants and young children. The tumor is characterized by the presence of a rhabdoid cell component in all cases, but the histological origin is still unclear. Recently, germline mutation of the *hSNF5/INI1* gene has been reported in association with AT/RTs.

The authors report a rare case of an intraocular AT/RT followed by a fourth ventricular tumor. The results of immunohistochemical studies of the surgical specimens revealed the presence of an AT/RT and from this finding the neural origin was inferred. A novel missense mutation of the *hSNF5/INI1* gene was demonstrated by DNA analysis. High-dose chemotherapy with stem cell rescue was effective in treating this patient. The immunohistochemical relationship between rhabdoid cells and the neurogenic zone, which has not been described in AT/RTs, is of great interest in view of the nature of rhabdoid cells.

KEY WORDS • atypical teratoid/rhabdoid tumor • germline mutation • *hSNF5/INI1* • subgranular zone • Musashi1 • nestin • pediatric neurosurgery

ATYPICAL AT/RTs are aggressive malignant tumors found in infants and young children. The prognosis is poor, despite the use of adjuvant therapy, and many patients die within a year following diagnosis.[3,13] The tumor is characterized by the presence of a rhabdoid cell component in all cases, variably mixed with other histological patterns including primitive neuroectodermal, mesenchymal, and epithelial components;[2,6,11,16,17] however, the histological origin is still unclear. Generally, monosomy or deletions from chromosome 22 have been identified in 60 to 90% of the cases.[3,13] The chromatin-remodeling gene *hSNF5/INI1* has recently been reported to act as a rhabdoid tumor suppressor gene,[18] and a germline mutation of *hSNF5/INI1* has been reported in malignant rhabdoid tumors, termed rhabdoid predisposition syndrome.[15]

The locations of AT/RTs vary; most arise in the posterior fossa (52%), followed by the supratentorial (39%), pineal (5%), multifocal (2%), and spinal (2%) areas.[10] Intraocular AT/RTs are rare. We report a case involving a neonate who presented with an intraocular tumor followed by an intramedullary tumor in the fourth ventricle.

Abbreviations used in this paper: AT/RT = atypical teratoid/rhabdoid tumor; MR = magnetic resonance; SGZ = subgranular zone.

Case Report

Patient History. This 5-week-old boy had been the product of a normal pregnancy and delivery. He did not appear to have medical problems and did not have a significant family history, but an abnormal left pupil was observed when the child was 2 weeks of age. An ophthalmological examination revealed a lesion appearing as a white mass behind the lens of his left eye. Ultrasonographic biomicroscopy and MR imaging around the orbit demonstrated an intraocular tumor, as demonstrated in Fig. 1. Because of the diagnostic uncertainty and little hope for useful vision, the patient was followed with observation alone; however, his left eye gradually enlarged and his general condition became worse. Ten months after the initial diagnosis, his left eye was enucleated because a histopathological examination revealed this tumor to be a rhabdoid cell tumor.

FIG. 1. Preoperative T_1- *(upper)* and T_2-weighted *(lower)* MR images of the left eye demonstrating a cone-shaped structure connecting the lens and posterior pole of the eye.

Operation. An extensive systemic workup demonstrated a fourth ventricular tumor of approximately 1.5 cm in diameter (Fig. 2). The patient immediately underwent a tumor resection via a suboccipital approach. The tumor was rather soft, relatively vascularized, and attached to the floor of the fourth ventricle. Gross-total resection of the tumor was achieved. Immunohistochemical studies of the surgical specimens from the eye and brain were consistent with AT/RT (Fig. 3, Table 1); DNA analysis revealed a germline *hSNF5/INI1* mutation (Fig. 4).

Postoperative Course. The patient received three courses of cisplatin at 90 mg/m^2 and etoposide at 300 mg/m^2, three courses of ifosfamide 9 g/m^2, carboplatin 1.5 g/m^2, and etoposide 450 mg/m^2, followed by two courses of vincristine 1.5 mg/m^2, nimustine 2 mg/m^2, and cisplatin 90 mg/m^2. The patient then underwent myeloablative chemotherapy with thiotepa 560 mg/m^2 and melphalan 130 mg/m^2 with stem cell rescue.[7,8] At last follow up, the boy had been free from recurrence or new occurrence of tumors for 24 months since the operation.

Histopathological Findings. Routine H & E staining of the intraocular tumor revealed that it consisted largely of necrotic tissues and hemorrhage, and that a small amount of tumor tissue remained. Tumor cells were large, pale, polygonal cells with distinct borders, vesicular nuclei, and moderate amounts of eosinophilic cytoplasm (Fig. 3 *upper left*), presenting a typical pattern of a rhabdoid cell tumor. The fourth ventricular tumor was composed mainly of poorly differentiated small and hyperchromatic cells resembling those of primitive neuroectodermal tumors and medulloblastomas, and it included rhabdoid cell components (Fig. 3 *upper right*). Both tumor cells demonstrated diffusely cytoplasmic positivity for cytokeratin AE1/AE3 and CAM-5.2, S100, vimentin, epithelial membrane antigen, and MIC2. Glial fibrillary acidic protein was expressed only in the brain tumor. Desmin, smooth-muscle actin, and HMB45 were not expressed. These results were used to aid in the diagnosis of both tumors as rhabdoid cell tumors. In addition, RNA-binding protein Musashi1 was expressed (Fig. 3 *lower left*) but nestin was not (Fig. 3 *lower right*) in both the intraocular and the fourth ventricular tumors; these proteins have been recently reported as markers for neural precursor cells.[9,14] The immunohistochemical results obtained with the different markers are summarized in Table 1.

Analysis of DNA. With the informed consent of his parents, genomic DNA was extracted from the peripheral blood of the patient and his parents as well as from the fourth ventricular tumor. Exons 1 to 9 of the *hSNF5/INI1* gene were amplified by polymerase chain reaction by using primers and conditions as previously described,[15] and the products of polymerase chain reaction were directly sequenced (Fig. 4). A novel heterozygous missense mutation of the *hSNF5/INI1* gene at codon 40 was identified from the peripheral blood of the patient's DNA. This mutation was considered de novo because no mutation was detected in his parents. In addition, the DNA analysis of the brain tumor showed only a mutated allele, suggesting a loss of het-

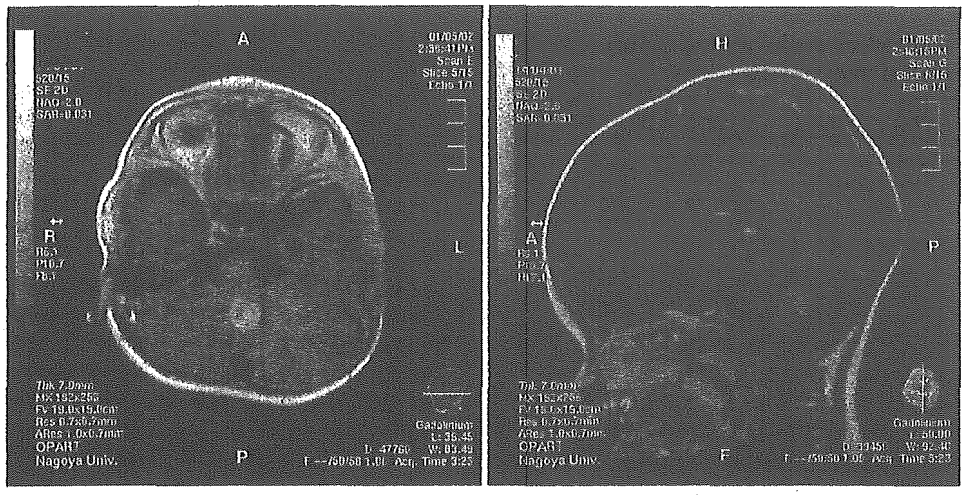

FIG. 2. Preoperative enhanced MR image of the brain demonstrating a fourth ventricular tumor with mass effect.

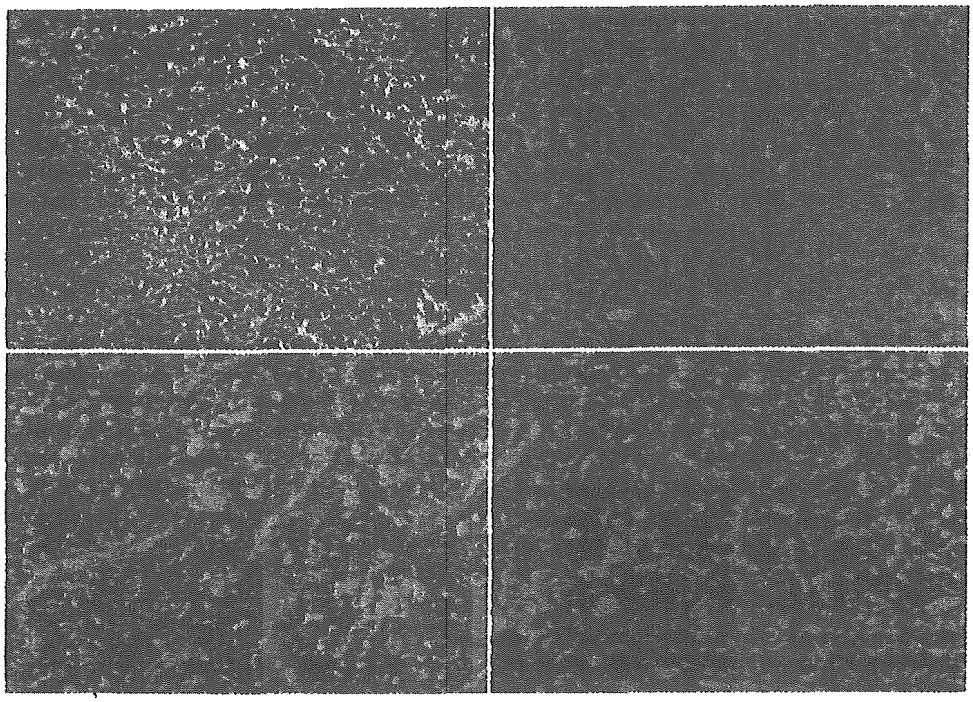

FIG. 3. Immunohistochemical studies demonstrating the intraocular tumor, the tissue of which is composed mainly of hematoma and necrosis, with tumor cells consisting of typical rhabdoid cells (*upper left*). The fourth ventricular tumor with poorly differentiated, small, hyperchromatic cells (*upper right*); the brain tumor with cytoplasmic positivity (*lower left*); the brain tumor specimen with limited positivity in vascular endothelial cells (*lower right*). H & E (*upper left* and *upper right*), Musashi1 (*lower left*), and nestin (*lower right*). Original magnifications × 200.

erozygosity. We could not analyze the intraocular tumor DNA because a limited amount of surgical specimens were available.

Discussion

Intraocular AT/RTs are extremely rare. Until now, there has been only one reported case in the literature of an intraocular malignant rhabdoid tumor that was believed to have metastasized from a renal tumor.[1] The relationship between intraocular and fourth ventricular tumors has not been clearly determined; however, the clinical course of the present case indicates that AT/RTs can possibly arise in the eyeball. Moreover, the germline mutation of *hSNF5/INI1* detected in this patient provides evidence of the multicentric origins of these tumors. The boy was thought to be suffering from a so-called rhabdoid predisposition syndrome, which is most likely to predispose a patient to a variety of cancers.[15]

TABLE 1

*Summary of the immunohistochemical findings of the intraocular and brain tumors**

Agent	Intraocular Tumor	Fourth Ventricular Tumor
cytokeratin		
AE1/AE3	+	+
CAM-5.2	+	+
S100	+	+
vimentin	+	+
EMA	+	+
MIC2	+	+
Musashi1	+	+
GFAP	−	+
SMA	−	−
desmin	−	−
HMB45	−	−
nestin	−	−

* EMA = epithelial membrane antigen; GFAP = glial fibrillary acidic protein; SMA = α–smooth muscle actin; + = positive; − = negative.

The phenotypic diversity of AT/RT cells is generally observed in tumor tissues; therefore, the histogenesis of AT/RT remains uncertain. Various cellular origins have been proposed, including neuroectodermal,[16] myogenic,[17] histiocytic,[6] neural,[2] and epithelial.[11] It may be inferred from these reports that an AT/RT has multiphenotypic characteristics, but the true origin of this enigmatic tumor is unknown. Recent studies involving normal neurons have established that neurogenesis of the brain persists in at least two discrete regions, the subventricular zone of the lateral ventricle[5] and the SGZ of the dentate gyrus.[4] Both nestin and the neural RNA-binding protein Musashi1 are expressed in neural stem cells in the subventricular zone.[9,14] In contrast, neuronal progenitor cells in the SGZ present with Musashi1 but not nestin.[16] In this case, Musashi1 was expressed but nestin was not in both the intraocular and the fourth ventricular tumors; these results indicate that these tumors might be derived from SGZ. Another hypothesis is that new peculiar cells are the origin for AT/RTs, although we cannot discuss this issue at present. As far as we are aware, this report provides the first documentation of a relationship between AT/RTs and the SGZ.

High-dose chemotherapy with stem cell rescue was effective in this case; however, the prognosis of AT/RTs is

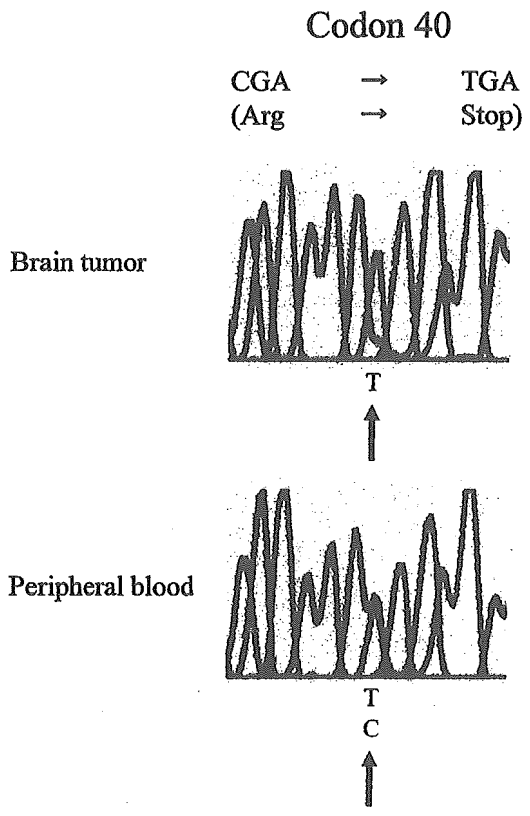

FIG. 4. Analysis of DNA revealing a missense mutation at codon 40 *(arrow)* in the brain tumor and peripheral blood specimens that predicts truncation of the protein. Control sequence obtained from the patient's parents is demonstrated below.

generally very poor. Even after aggressive surgery and chemotherapy, overall survival rates for children, particularly for those younger than 2 years of age, have been extremely poor, with less than 20% of patients surviving less than 12 months from the time of diagnosis.[3,13] A variety of different chemotherapeutic agents have been used, but no single agent or combination of agents have been shown to be most effective. Ronghe, et al.,[12] recently reported the effectiveness of intensified therapy for AT/RTs. More consideration is needed to develop a new therapeutic strategy for these types of tumors.

Conclusions

We report a rare case of an intraocular AT/RT followed by a fourth ventricular tumor. Immunohistochemical studies indicated the neural origin of these tumors. High-dose chemotherapy with stem cell rescue was an effective treatment in this case.

References

1. Akhtar M, Ali MA, Sackey K, Bakry M, Johnson T: Malignant rhabdoid tumor of the kidney presenting as intraocular metastasis. **Pediatr Hematol Oncol 8:**33–43, 1991
2. Bonnin JM, Rubinstein LJ, Palmer NF, Beckwith JB: The association of embryonal tumors originating in the kidney and in the brain. A report of seven cases. **Cancer 54:**2137–2146, 1984
3. Burger PC, Yu IT, Tihan T, Friedman HS, Strother DR, Kepner JL, et al: Atypical teratoid/rhabdoid tumor of the central nervous system: a highly malignant tumor of infancy and childhood frequently mistaken for medulloblastoma: a Pediatric Oncology Group study. **Am J Surg Pathol 22:**1083–1092, 1998
4. Gage FH, Kempermann G, Palmer TD, Peterson DA, Ray J: Multipotent progenitor cells in the adult dentate gyrus. **J Neurobiol 36:**249–266, 1998
5. Garcia-Verdugo JM, Doetsch F, Wichterle H, Lim DA, Alvarez-Buylla A: Architecture and cell types of the adult subventricular zone: in search of the stem cells. **J Neurobiol 36:** 234–248, 1998
6. Gonzalez-Crussi F, Goldschmidt RA, Hsueh W, Trujillo YP: Infantile sarcoma with intracytoplasmic filamentous inclusions: distinctive tumor of possible histiocytic origin. **Cancer 49:** 2365–2375, 1982
7. Guruangan S, Dunkel IJ, Goldman S, Garvin JH, Rosenblum M, Boyett JM, et al: Myeloablative chemotherapy with autologous bone marrow rescue in young children with recurrent malignant brain tumors. **J Clin Oncol 16:**2486–2493, 1998
8. Heideman RL, Packer RJ, Reaman GH, Allen JC, Lange B, Horowitz ME, et al: A phase II evaluation of thiotepa in pediatric central nervous system malignancies. **Cancer 72:** 271–275, 1993
9. Kaneko Y, Sakakibara S, Imai T, Suzuki A, Nakamura Y, Sawamoto K, et al: Musashi1: an evolutionally conserved marker for CNS progenitor cells including neural stem cells. **Dev Neurosci 22:**139–153, 2000
10. Kleihues P, Louis DN, Scheithauer BW, Rorke LB, Reifenberger G, Burger PC, et al: The WHO classification of tumors of the nervous system. **J Neuropathol Exp Neurol 61:** 215–229, 2002
11. Parham DM, Peiper SC, Robicheaux G, Ribeiro RC, Douglass EC: Malignant rhabdoid tumor of the liver. Evidence for epithelial differentiation. **Arch Pathol Lab Med 112:**61–64, 1988
12. Ronghe MD, Moss TH, Lowis SP: Treatment of CNS malignant rhabdoid tumors. **Pediatr Blood Cancer 42:**254–260, 2004
13. Rorke LB, Packer R, Biegel J: Central nervous system atypical teratoid/rhabdoid tumors of infancy and childhood. **J Neurooncol 24:**21–28, 1995
14. Sakakibara S, Imai T, Hamaguchi K, Okabe M, Aruga J, Nakajima K, et al: Mouse-Musashi-1, a neural RNA-binding protein highly enriched in the mammalian CNS stem cell. **Dev Biol 176:**230–242, 1996
15. Sevenet N, Sheridan E, Amram D, Schneider P, Handgretinger R, Delattre O: Constitutional mutations of the *hSNF5/INI1* gene predispose to a variety of cancers. **Am J Hum Genet 65:** 1342–1348, 1999
16. Suzuki A, Ohta S, Shimada M: Gene expression of malignant rhabdoid tumor cell lines by reverse transcriptase-polymerase chain reaction. **Diagn Mol Pathol 6:**326–332, 1997
17. Tsokos M, Kouraklis G, Chandra RS, Bhagavan BS, Triche TJ: Malignant rhabdoid tumor of the kidney and soft tissues. Evidence for a diverse morphological and immunocytochemical phenotype. **Arch Pathol Lab Med 113:**115–120, 1989
18. Vujanic GM, Sandstedt B, Harms D, Boccon-Gibod L, Delemarre JF: Rhabdoid tumor of the kidney: a clinicopathological study of 22 patients from the International Society of Paediatric Oncology (SIOP) nephroblastoma file. **Histopathology 28:** 333–340, 1996

Manuscript received April 26, 2004.
Accepted in final form October 21, 2004.

Address reprint requests to: Jun Yoshida, M.D., Ph.D., Department of Neurosurgery, Nagoya University Graduate School of Medicine, 65, Tsurumai-cho, Showa-ku, Nagoya 466–8550, Japan. email: jyoshida@med.nagoya-u.ac.jp.

ELSEVIER

Neoplasm

THE COMBINATION OF MITOTIC AND KI-67 INDICES AS A USEFUL METHOD FOR PREDICTING SHORT-TERM RECURRENCE OF MENINGIOMAS

Jun A. Takahashi, M.D.,* Tetsuya Ueba, M.D.,* Nobuo Hashimoto, M.D.,* Yasuaki Nakashima, M.D.,† and Naomi Katsuki, M.D.†

**Department of Neurosurgery, and †Laboratory of Anatomic Pathology, Kyoto University Graduate School of Medicine, Kyoto, Japan*

Takahashi JA, Ueba T, Hashimoto N, Nakashima Y, Katsuki N. The combination of mitotic and Ki-67 indices as a useful method for predicting short-term recurrence of meningiomas. Surg Neurol 2004;61:149–56.

BACKGROUND

The most relevant factor in the progression-free survival (PFS) of patients with meningiomas is the malignant grade. However, using only the current World Health Organization (WHO) definition that does not consider precise quantitative indicators, an unequivocal diagnosis of the malignant grade is difficult. In our retrospective study of the PFS of meningioma patients, we focused on mitoses and the Ki-67 staining index of tumor specimens obtained at the initial surgery.

METHODS AND RESULTS

A total of 349 patients with intracranial meningioma, operated between 1978 and 2000, were followed for a mean of 7 years. According to the mitotic index (MI), we classified them into 3 groups. In Group A (n = 326), slide-mounted tumor samples exhibited no mitoses; in Group B (n = 15) there were fewer than 4 mitoses, and in Group C (n = 8) 4 or more mitoses were seen per 10 high-power fields (HPF). The estimated 5-year PFS rates in Groups A, B, and C were 93%, 10%, and 13% respectively. The mean PFS for Group A was 148 months; in Groups B and C the median PFS was 43 and 16 months, respectively. A Ki-67 staining index (SI) of less than 1% corresponded with no mitosis, while an SI exceeding 5% was indicative of the presence of mitoses.

CONCLUSION

In meningioma patients, no mitoses and/or a Ki-67 SI <1% signals a favorable outcome. An SI >5% or the presence of mitoses, even fewer than 4 in 10 HPF, is suggestive of a short PFS irrespective of other pathologic features. We suggest that in combination, assay of the Ki-67 SI and the MI represents a reliable, quantitative tool for predicting PFS in meningioma patients. © 2004 Elsevier Inc. All rights reserved.

Address reprint requests to: Jun A. Takahashi, M.D., Department of Neurosurgery, Kyoto University Graduate School of Medicine, 54 Shogoin-Kawahara-cho, Sakyo-ku, Kyoto 606–8507, Japan.

Received November 19, 2002; accepted June 12, 2003.

KEY WORDS

Meningioma, Ki-67 staining index, mitotic index, progression-free survival.

Although meningiomas are generally slow-growing, benign tumors, 20% of gross-totally resected meningiomas recur within 20 years [14]. The most relevant factor for progression-free survival (PFS) is their histologic malignant grade: while approximately 7 to 20% of benign meningiomas recur, for atypical- and anaplastic meningiomas the recurrence rates are much higher at 29 to 40% and 50 to 78%, respectively [7,9,11,14,16,24,25]. Thus, while the value of histologic grading is obvious, their objective staging has been hampered by the fact that the World Health Organization (WHO) classification of meningiomas relies heavily on qualitative criteria without taking into account more precise quantitative indicators such as numerical scoring systems.

The mitotic index (MI) is only one numerical criterion of pathologic grades in the WHO classification of meningiomas [14]. For the purpose of diagnosing atypical and anaplastic meningiomas, increased mitotic activity is defined as the presence of 4 or more and 20 or more mitoses per 10 high-power fields (HPF), respectively. Proliferation indices as well as the MI are significantly correlated with tumor-doubling time [14,20] and a Ki-67 staining index (SI) of more than 5 to 10% reflects an increased risk of recurrence as well as a high grade of malignancy [14]. In typical cases with obvious pathologic features of malignancy, increased mitotic activity, and a Ki-67 SI far exceeding the cut-off value, an unfavorable outcome is easily predicted at the time of the initial surgery. However, the prognosis varies in patients with meningiomas that lack

© 2004 Elsevier Inc. All rights reserved.
360 Park Avenue South, New York, NY 10010–1710

0090-3019/04/$–see front matter
doi:10.1016/S0090-3019(03)00575-5

the typical malignant features and exhibit few mitoses and a Ki-67 SI near the cut-off level.

In this retrospective study of 349 patients with surgically removed intracranial meningiomas, we assessed the correlation between the MI and the clinical outcome represented by their PFS. We paid special attention to the prognostic significance of the presence of any mitotic figures in tumor tissue samples obtained at the time of the initial operation. As we detected a relationship between the Ki-67 SI and the presence of even fewer than 4 mitoses/10 HPF, we now suggest that in combination, these two parameters represent a powerful and quantitative tool for predicting PFS even in some meningiomas that are not easily classified into a benign or atypical type according to the WHO criteria.

SUBJECTS AND METHODS

PATIENT POPULATION

Between 1978 and 2000, 426 patients with intracranial meningiomas underwent surgical treatment at Kyoto University Hospital. Their medical records were carefully reviewed and all clinical, laboratory, radiographic, pathologic, and follow-up data were retrieved. Of the 426 patients, 349 were entered into this study because they fulfilled all of the following criteria: 1) they had undergone no previous surgical treatment of their tumors, 2) their postoperative follow-up exceeded 1 year, and 3) they did not have meningeal hemangiopericytoma. Before tumor recurrence, none of the 349 patients had received radiation therapy.

There were 118 males and 231 females; their mean age was 54 years (range 18 to 78 years). Diagnosis was based on hematoxylin-eosin (H&E) staining of tumor samples from the initial surgery; of the 349 meningiomas, 331 (94.8%) were benign, 16 (4.6%) were atypical, and 2 (0.6%) were anaplastic. According to WHO criteria, we made a diagnosis of atypical or anaplastic type based on whether the tumor samples manifested a MI of 4 or more or 20 or more mitoses per 10 high-power fields (HPF), respectively, as well as pathologic findings such as increased cellularity, small cells with a high nucleus: cytoplasm ratio, prominent nucleoli, uninterrupted patternless or sheet-like growth, and foci of necrosis [14].

We used the system of Simpson [28] to record the extent of tumor removal. Accordingly, 118 patients (33.8%) had undergone Grade I resection (complete with excision of the dural insertion), 150 (43.0%) Grade II (complete with coagulation of the dural insertion), 53 (15.2%) Grade III (incomplete, leaving behind a small amount of tumor tissue), and 28 (8.0%) Grade IV (incomplete, with a large amount of residual tumor tissue). Of the 326 Group A patients, 110 (33.7%) had undergone Simpson's grade I resection, 146 (44.8%) Grade II, 46 (14.1%) Grade III, and 24 (7.4%) Grade IV. Of the 15 Group B patients, 5 (33.3%) had received Grade I resection, 2 (13.3%) Grade II, 4 (26.7%) Grade III, and 4 (26.7%) Grade IV. Of the 8 Group C patients, 3 (37.5%) had undergone Grade I resection, 2 (25%) Grade II, 3 (37.5%) Grade III, and none Grade IV. The extent of resection was deduced from the recorded description of the operation and confirmed by inspecting postoperative computed tomography (CT) and/or magnetic resonance (MR) images in the patients' medical records. Other clinicoradiological findings such as perifocal edema, tumor staining, feeding from pial arteries, tumor hardness, arachnoid penetration, tumor demarcation, and tumor location were also confirmed by inspection of the surgical records and/or neuroradiological images.

During a mean follow-up time of 83 months (range 12–253 months), 42 of the 349 patients (12.0%) experienced recurrence; of these, 31 (73.8%) had benign- and the remaining 11 had atypical- or anaplastic meningiomas. The criteria for diagnosing recurrence were the demonstration, during regular follow-up, MR and/or CT evidence of tumor appearance after complete resection, or of regrowth of residual tumors.

ASSESSMENT OF THE MI AND THE KI-67 SI

In all 349 patients, tumor tissues obtained at the first operation were subjected to MI determination. The specimens were fixed with formalin, embedded in paraffin, and tissue samples mounted on slides were stained with H&E. The MI was determined by counting the number of unequivocal mitotic figures in 10 consecutive HPF (× 400) containing the highest number of mitoses [25].

In 29 of 42 patients with tumor recurrence, the Ki-67 SI of tumor tissues obtained at the first operation was additionally determined. Tissue sections (4 μm in thickness) were deparaffinized and immunostained using the Ventana NX automated immunohistochemistry system (Ventana Medical Systems, Tucson, AZ). Briefly, the slides were heated in a 750W microwave oven (5 min × 4) in citrate buffer (pH 6) and then incubated for 1 hour with anti-Ki-67/MIB-1 (Dako, Carpenteria, CA) diluted 1:100 in bovine serum albumin/TBS. Immunoreactions were then performed according to the LSAB method using streptavidin-biotin complex (ABC)-labeled horseradish peroxidase and diaminobenzidine

(DAB). All tissue sections were examined at high-power magnification (× 400). The number of cells stained positively with anti-Ki-67 antibody and the total number of tumor cells were counted in several representative fields containing more than 1000 cells and their ratio was expressed as the Ki-67 SI (%) [20]. In areas with heterogeneous distribution of Ki-67 immunopositive cells, the area containing the largest number of Ki-67-stained cells was considered to represent the proliferative activity of the tumor.

Using the H&E-stained sections, 2 pathologists (NK, YN) independently made the histologic diagnosis and graded the tumors. They inspected H&E-stained or immunostained sections together, using a multi-head microscope, and assigned the MI and Ki-67 SI by consensus. Although they were cognizant of the diagnosis, they made their assessments before accessing any information pertaining to the outcomes.

STATISTICAL ANALYSIS

The relationship between the MI and the Ki-67 SI was examined by the Pearson correlation coefficient. In addition, PFS curves were prepared using the Kaplan-Meier method. The log-rank test was employed to determine whether the MI-based classification, the extent of surgical resection, the pathologic diagnosis, and other clinicoradiological parameters were associated in a univariate manner with PFS. Differences were considered statistically significant at $p < 0.05$.

RESULTS

CLINICAL OUTCOMES AND MI

The 349 meningioma patients were divided into 3 groups according to their MI. Group A (no mitoses) consisted of 326 patients (322 benign-, 4 atypical meningiomas), Group B (more than 0 and fewer than 4 mitotic figures/10 HPF) of 15 (9 benign, 6 atypical or anaplastic), and Group C (4 or more mitotic figures/10 HPF) of 8 patients with atypical or anaplastic meningioma. There were no cases with 20 or more mitotic figures per 10 HPF.

The 349 patients were followed for a mean of 83 months. As shown in Figure 1A, the estimated 5-year PFS rates in Groups A, B, and C were 93%, 10%, and 13%, respectively. The mean PFS for Group A was 148 months; in Groups B and C the median PFS was 43 and 16 months, respectively. By the log-rank analysis, the difference in PFS between Group A and the other 2 groups was significant (Group A vs. B, $p < 0.0001$; A vs. C, $p < 0.0001$; A vs.

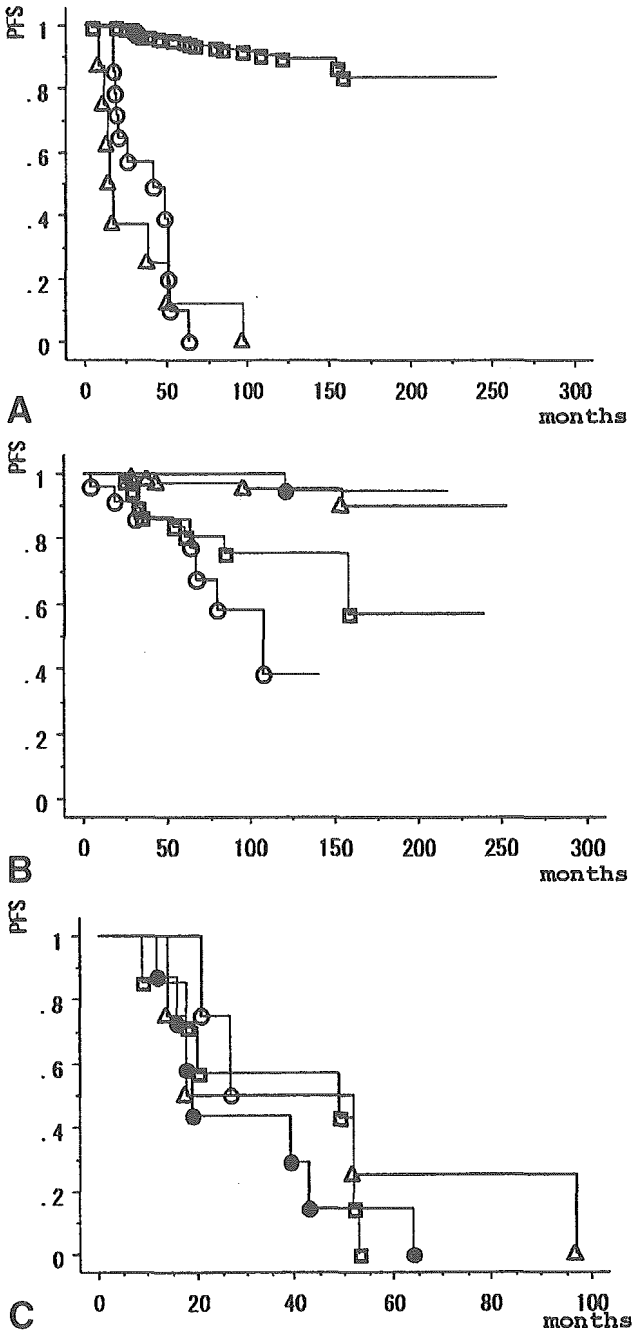

1 (A) Kaplan-Meier curves of progression-free survival (PFS) in patients grouped according to the mitotic index (MI) of surgical tumor specimens. Open squares, Group A (no mitotic figures); open circles, Group B (more than 0 and fewer than 4 mitotic figures per 10HPF); open triangles, Group C (more than 4 mitotic figures per 10HPF). (**B**) Kaplan-Meier curves of PFS in Group A patients classified according to the Simpson resection grade. Solid circles, Grade I; open triangles, Grade II; open squares, Grade III; open circles, Grade IV. For a description of Simpson grades, see Subjects and Methods. (**C**) Kaplan-Meier curves of PFS in Group B and C patients classified according to the Simpson resection grade. For symbols, see Figure 1**B**.

1 Correlation Analyses of Clinicopathological Factors With Recurrence

	Frequency (%)	Overall Cases	Group A	Group B	Group C	Group B+C
Mitoses (+)	7%	<0.0001				
Simpson Grades		<0.0001	<0.0001	NS	NS	NS
Simpson I or II	78	<0.0001	<0.0001	NS	NS	NS
Perifocal edema on MR images (+)	46	NS	0.009	NS	NS	NS
Hard tumors	48	NS	NS	NS	NS	NS
Arachnoid penetration (+)	26	NS	NS	NS	NS	NS
Well-demarcated tumors	96	0.01	0.006	NS	NE	NS
Tumor stain on angiograms (+)	75	NS	0.03	NS	NS	NS
Feeding from pial arteries on angiogram	28	NS	NS	NS	NE	NS
Tumor locations		0.03	0.0002	NS	NS	NS
Tumors located on skull base	48	0.01	<0.0001	NS	NS	NS

Frequency is calculated in overall cases.
Cases with no mitoses, those with 1–4 mitoses per 10HPF, and 4 or more mitoses per 10 HPF are present in each of the 3 groups.
NS = not significant, NE = not examined because of insufficient numbers of cases.

B and C combined, $p < 0.0001$). Group B and C did not significantly differ with respect to PFS ($p = 0.3945$).

The frequencies of radiologic, operative, and pathologic findings and their univariate associations are summarized in Table 1. In the analysis of overall cases and of Group A patients, parameters such as the Simpson grade, tumor demarcation, and tumor location contributed to variability in the Kaplan-Meier PFS curves assessed by the log-rank test. In contrast, none of the variables examined significantly affected the PFS curves of Group B and C, nor of Groups B and C combined.

Figure 1B shows the Kaplan-Meier PFS curves for all 326 Group A patients classified according to the Simpson resection grades. The estimated 5-year PFS rates for Simpson Grades I, II, III, and IV were 100%, 97%, 81%, and 77%, respectively; the 10-year PFS rates were 95%, 93%, 76%, and 38%; and the mean PFS was 121, 150, 132, and 85 months. According to the log-rank test, in Group A, the Simpson grade had a significant effect on PFS: the greater the extent of resection, the longer was the PFS and the lower the progression ratio ($p < 0.0001$). On the other hand, in Groups B and C, the extent of resection had no significant impact on PFS ($p = 0.71$) (Figure 1C). The estimated 2-year PFS rates for the 23 patients in Groups B and C who had undergone Grade I, II, III, or IV resection were 42%, 50%, 57%, and 75%, respectively; the median PFS was 19, 18, 49, and 6 months. In Group B alone and Group C alone, there was also no significant association of the Simpson's grade with PFS ($p = 0.97$ and $p = 0.58$, respectively).

KI-67 SI AND MI

In 29 of the 42 patients with recurrence we determined the Ki-67 SI in tumor samples from the initial surgery. The mean Ki-67 SI values ± SD were 1.5 ± 1.2 in Group A ($n = 14$), 6.7 ± 4.3 in Group B ($n = 9$), and 12.8 ± 6.5 in Group C ($n = 6$). Based on the Pearson correlation coefficient, there was a significant correlation between the MI and the Ki-67 SI ($r = 0.81$, $p < 0.0001$). Figure 2 shows that all cases with a Ki-67 SI below 1% were from Group A. An SI exceeding 5% was indicative of the presence of mitoses (Groups B and C). Patients from all groups could be found in the 1 to 5% SI range.

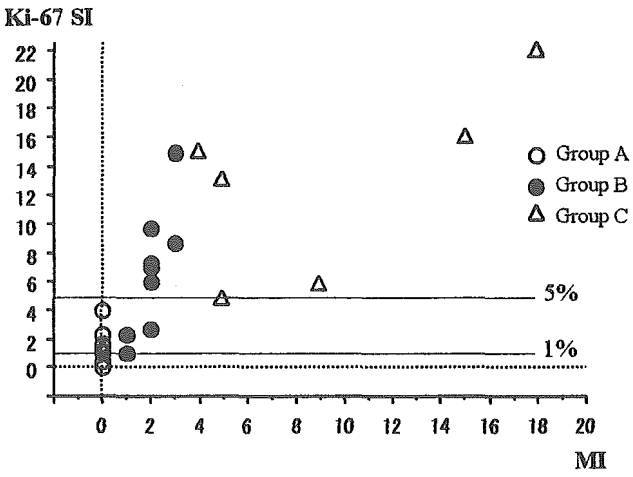

2 Correlation of mitotic index with Ki-67 staining index. Open circles, Group A (no mitotic figures); closed circles, Group B (more than 0 and fewer than 4 mitotic figures per 10HPF); open triangles, Group C (more than 4 mitotic figures per 10HPF).

COMPARISON BETWEEN THE MI AND PATHOLOGIC DIAGNOSIS

The 331 patients with a pathologic diagnosis of benign meningioma manifested an estimated 5-year PFS rate of 91% with a mean PFS of 144 months. On the other hand, in the 18 patients with atypical or anaplastic meningiomas, the estimated 5-year PFS rate was 32% with a median PFS of 52 months. Kaplan-Meier analysis showed that the difference in PFS between benign and atypical/anaplastic meningiomas was significant ($p < 0.0001$). The Simpson grade had a significant effect on PFS only in the 331 patients with benign meningiomas ($p < 0.001$); the estimated 5-year PFS rates for Grades I, II, III, and IV were 97%, 95%, 95%, and 90%, respectively; the 10-year rates were 76%, 70%, 80%, and 35%; and the mean PFS was 117, 148, 126, and 82 months.

In Group A, none of the 4 meningiomas designated atypical according to WHO criteria (MI = 0) recurred during a mean follow-up of 61 months. On the other hand, all 9 benign meningiomas in Group B recurred after a mean of only 38 months (range 18–64 months), a shorter interval than we expected for ordinary benign meningiomas.

DISCUSSION

Although meningiomas are generally benign, slow-growing tumors with apparent demarcation, they have a tendency to recur after a period of more than 10 years [14,28]. Putative prognostic factors are age, attachment to intracranial structures (location), the extent of resection [7,8,28], grade of malignancy [9,25], and proliferation indices [6,10–15,17,18,20,21]. The pathologic grade of malignancy has been proposed as the most relevant overall predictor of recurrence [14]. However, there are patients whose tumors are not pathologically identifiable as benign or atypical because the grade of malignancy cannot be unequivocally determined. The WHO classification proposes primarily qualitative criteria for defining grades of malignancy; except for the MI, it does not provide more precise quantitative indicators that could be assessed according to numerical scoring systems. For the purpose of diagnosing atypical meningiomas, the WHO criteria define increased mitotic activity as the presence of 4 or more mitoses per 10 HPF. However, with respect to assigning a malignant grade to meningiomas, the WHO classification system does not consider a finding of fewer than 4 mitoses of importance [14].

Proliferation indices such as the Ki-67 SI are useful for predicting tumor recurrence and survival. While previous studies documented that the Ki-67 SI significantly correlates with the pathologic grade of meningiomas, there is considerable variation in the Ki-67 SI values reported in different studies and by different institutions. In fact, the reported mean values for benign-, atypical-, and anaplastic meningiomas range widely between 0.7 and 3.8%, 2.1 and 7.1%, and 10.9 and 14.7%, respectively [1,10,14,15,21,26,27]. Moreover, some reports suggested significant overlapping of Ki-67 values among various pathologic grades of malignancy [1,6,12,13]. Perry et al [25] who performed statistical analyses of 62 meningioma cases, suggested that a Ki-67 SI of 4.2% represented a threshold and that an SI in excess of 4.2% was indicative of high tumor proliferation activity. Although we agree that values markedly above or below this threshold may signal unfavorable and favorable outcomes respectively, in view of the wide range of reported Ki-67 SI values, we favor the establishment of stricter SI criteria to predict clinical outcomes.

In efforts to develop a system whereby quantitative indicators can be used to predict the PFS of meningioma patients, we performed the current retrospective study. We assessed whether the combination of an MI that confirms the presence of even fewer than 4 mitoses per 10 HPF and the KI-67 SI is of prognostic significance. Surgically removed meningioma tissues in 326 of 349 patients (93.4%) exhibited no evidence of mitosis. In most of the remaining 23 tissue samples the MI was around 4 per 10 HPF; none of the patients had an MI of more than 20. We found that compared to the other 2 groups, in patients with no mitoses (Group A), the 5-year incidence of tumor progression was lower (7%) and the mean PFS longer (148 months), and that the Simpson grade had a significant effect on PFS. Group B (more than 0 and fewer than 4 mitoses) and Group C patients (MI of 4 or more) had higher 5-year recurrence rates at 90% and 87%, respectively, and shorter PFS (median 43 and 16 months, respectively). A Ki-67 SI of less than 1% corresponded with the absence of mitoses in the tumor samples (Group A), while an SI exceeding 5% reflected the presence of mitotic figures (Groups B and C). Therefore, we propose that SI values of 1% and 5% be used as threshold values for predicting favorable and unfavorable outcomes, respectively, in meningioma patients. Patients from all 3 groups were found in the SI value range from 1 to 5%, therefore, a Ki-67 SI in this range is not a reliable, independent predictive indicator of the outcome. Assessment of the Ki-67 SI is relatively easy com-

pared to the calculation of a low MI whose determination is complex. Although the Ki-67 SI alone is generally used for predicting the outcome in meningioma patients, we stress the need for determining the MI, especially in patients whose Ki-67 SI is in the 1 to 5% range.

Patients with atypical and anaplastic meningiomas diagnosed according to the current WHO criteria had higher recurrence rates and shorter PFS than did patients with benign tumors. This finding coincides with the difference we observed in the MI of Group A patients and the MI in Groups B and C. It is important to note that none of the 4 atypical meningiomas in Group A manifested recurrence during a mean follow-up period of 61 months whereas all 9 benign meningiomas in Group B recurred after a mean of only 38 months (range 18–64 months). The time to recurrence of these benign tumors was shorter than we would have expected. In some of our patients the clinical outcome was at variance with the expected outcome based on the malignancy grade determined by WHO criteria. We found that in such patients, the MI reflected the likelihood of short-term recurrence much better than did the malignant grade. In addition, although an MI of 4 or more per 10 HPF is the consensus criterion for atypical meningiomas, our results suggest that a small number of mitoses, even fewer than 4 per 10 HPF, is also an important indicator for predicting the short-term progression of meningiomas.

Atypical and anaplastic meningiomas tend to recur within a short period even after gross total removal. Patients with these meningioma types require repeated operations and some have been treated with postoperative extrabeam radiation therapy (EBRT) although high-grade meningiomas are usually refractory to EBRT [2–4,19,23]. In these meningiomas, stereotactic radiosurgery (SRS) as a boost to EBRT, as salvage therapy after EBRT, or instead of EBRT, has yielded disappointing results. In atypical meningiomas the 5-year local control and 5-year overall survival rates were 32 to 48% and 83 to 95%, respectively; in anaplastic meningiomas they were 0 to 34% and 21.5 to 60% [5,22,23]. As the tumor control rate following SRS was better in patients with small (< 8 cm^3) malignant meningiomas [22], we stress that early diagnosis and immediate treatment of small recurrent tumors is imperative for improving the outcomes of patients with atypical and anaplastic meningiomas. We need a method that allows us to predict the PFS in all meningioma patients so that postoperative therapy can be selected on a case-by-case basis.

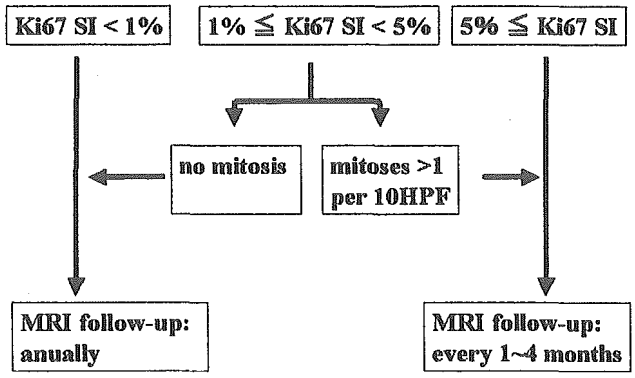

3 Proposal schedule of postoperative follow-up MRI based on MI and Ki-67 SI.

CONCLUSION

Our retrospective study of 349 patients with surgically treated meningiomas revealed that numerical scoring systems, i.e., the Ki-67 SI and the MI, determined at the time of the initial operation, make possible the prediction of long or short PFS. Based on our results, we propose that tumors with a Ki-67 SI of less than 1% be followed as benign meningiomas and subjected to annual MRI study (Figure 3). On the other hand, surgical specimens with a Ki-67 SI greater than 5% should be monitored as atypical or anaplastic meningiomas and undergo follow-up MRI study at intervals of a few months. In cases where the Ki-67 SI is between 1 and 5%, we suggest that the MI of tumor tissue samples be carefully determined. If there is no evidence of mitoses, annual MRI study should be performed. However, patients with even a few mitotic figures should be followed by MRI at shorter intervals.

Our retrospective analysis of 349 surgically treated meningioma patients revealed that the presence of mitotic figures in tumor tissues obtained at the first operation correlated with shorter PFS when compared to patients whose specimens contained no mitotic figures. We also determined that the threshold for predicting favorable and unfavorable treatment outcomes with the Ki-67 SI are 1% and 5%, respectively. In meningiomas with a Ki-67 SI between 1% and 5%, the presence of mitoses, even less than 4 in 10 HPF, is indicative of an increased risk for recurrence. The combination of the Ki-67 SI and the MI represents a convenient and quantitative tool for predicting PFS. We posit that in cases where a diagnosis of malignant meningioma is based on current WHO criteria, these combined assays make possible a more precise prediction of the prognosis.

REFERENCES

1. Abramovich C, Prayson RA. MIB-1 labelling indices in benign, aggressive, and malignant meningiomas: a study of 90 tumors. Hum Pathol 1998;29:1420–7.
2. Chamberlain MC. Adjuvant combined modality therapy for malignant meningiomas. J Neurosurg 1996;84:733–6.
3. Glaholm J, Bloom HJG, Crow JH. The role of radiotherapy in the management of intracranial meningiomas: the Royal Marsden hospital with 186 patients. Int J Radiat Oncol Biol Phys 1989;18:735–61.
4. Goyal LK, Suh JH, Mohan DS, Prayson RA, Lee J, Barnett GH. Local control and overall survival in atypical meningioma: a retrospective study. Int J Radiat Oncol Biol Phys 2000;46:57–61.
5. Hakim R, Alexander E III, Loeffler JS, et al. Results of linear accelerator-based radiosurgery for intracranial meningiomas. Neurosurgery 1998;42:446–54.
6. Hsu DW, Efird JT, Hedley WET. MIB-1 (Ki-67) index and transforming growth factor-alpha (TGF alpha) immunoreactivity are significant prognostic predictors for meningiomas. Neuropathol Appl Neurobiol 1998;24:441–52.
7. Jaaskelainen J, Haltia M, Laasonen E, Wahlstrom T, Valtonen S. The growth rate of intracranial meningiomas and its relation to histology. Surg Neurol 1985; 24:165–72.
8. Jellinger K, Slowik F. Histological subtypes and prognostic problems in meningiomas. J Neurol 1975;208: 279–98.
9. Kallio M, Sankila R, Hakulinen T, Jaaskeleinen J. Factors affecting operative and excess long-term mortality in 935 patients with intracranial meningioma. Neurosurgery 1992;31:2–12.
10. Karamitopoulou E, Perentes E, Tolnay M, Probst A. Prognostic significance of MIB-1, p53, and bcl-2 immunoreactivity in meningiomas. Hum Pathol 1998;29: 140–5.
11. Kolles H, Niedermayer I, Schmitt C, et al. Triple approach for diagnosis and grading of meningiomas: histology, morphometry of Ki-67/Feulgen stainings, and cytogenesis. Acta Neurochir Wien 1995;137:174–81.
12. Konstantinidou AE, Patsouris E, Korkolopoulou Kavantazas N, Mahera H, Davaris P. DNA topoisomerase IIa expression correlates with cell proliferation but not with recurrence in intracranial meningiomas. Histopathol 2001;39:402–8.
13. Lanzafame S, Torrsi A, Barbagallo G, Emmanuele C, Alberio N, Albanese V. Correlation between histological grade, MIB-1, p53, and recurrence in 69 completely resected primary intracranial meningiomas with a 6 year mean follow-up. Pathol Res Pract 2000; 196:483–8.
14. Louis DN, Scheithauer BW, Budka H, von Deimling A, Kepes JJ. Meningiomas. In: Kleihues P, Cavenee K, eds. WHO Classification of Tumors, Pathology & Genetics, Tumours of the Nervous System. Lyon: IARC press, 2000:176–84.
15. Madsen C, Shroder HD. Ki-67 immunoreactivity in meningiomas: determination of the proliferative potential of meningiomas using the monoclonal antibody Ki-67. Clin Neuropathol 1997;16:137–42.
16. Maier H, Ofner D, Hittmair A, Kitz K, Budka H. Classic, atypical, and anaplastic meningioma: three histopathological subtypes of clinical subtypes of clinical relevance. J Neurosurg 1992;77:616–23.
17. Maier H, Wanschitz Sedivy R, Rossler K, Ofner D, Budka H. DNA fragmentation in meningioma subtypes. Neuropathol Appl Neurobiol 1997;23:496–506.
18. Matsuno A, Fujimaki T, Sakaki T, et al. Clinical and histopathological analysis of proliferative potentials of recurrent and non-recurrent meningiomas. Acta Neuropathol 1996;91:504–10.
19. Milosevic MF, Frost PJ, Laperriere NJ, Wong CS, Simpson WJ. Radiation for atypical or malignant intracranial meningioma. Int J Radiat Oncol Biol Phys 1996; 34:817–22.
20. Nakaguchi H, Fujimaki T, Matsuno A, et al. Postoperative residual tumor growth of meningioma can be predicted by MIB-1 immunohistochemistry. Cancer 1999;85:2249–54.
21. Nakasu S, Nakajima M, Matsumura K, Nakasu Y, Handa J. Meningiomas: proliferating potential and clinicoradiological features. Neurosurgery 1995;37: 1049–55.
22. Ojemann SG, Sneed PK, Larson DA, et al. Radiosurgery for malignant meningioma: result in 22 patients. J Neurosurg 2000;93(suppl 3):62–7.
23. Palma L, Celli P, Franco C, Cervoni L, Cantore G. Long-term prognosis for atypical and malignant meningiomas: a study of 71 surgical cases. J Neurosurg 1997;86:793–800.
24. Perry A, Stafford SL, Scheithauer BW, Suman VJ, Lohse CM. Meningioma grading: analysis of histologic parameters. Am J Surg Pathol 1997;21:1455–65.
25. Perry A, Scheithauer BW, Stafford SL, Lohse CM, Wollan PC. Malignancy in meningiomas: a clinicopathological study of 116 patients, with grading implications. Cancer 1999;85:2046–56.
26. Prayson RA. Malignant meningioma: a clinicopathologic study of 23 patients including MIB-1 and p53 immunohistochemistry. Am J Clin Pathol 1996;105: 719–26.
27. Sandberg DI, Edger MA, Resch L, Ruthka JT, Becker LE, Souweidane MM. MIB-1 staining index of pediatric meningiomas. Neurosurgery 2001;48:590–7.
28. Simpson D. The recurrence of i. c. meningiomas after surgical treatment. J Neurol Neurosurg Psychiat 1957; 20:22–39.